QCD in DIS at HERA

Gregorio Bernardi
LPNHE - Paris

on behalf of the

H1 and ZEUS Collaborations

SLAC - Topical Conference, 12^{th} of August 1998

Many thanks to my H1 and ZEUS colleagues, in particular
to Ursula Bassler, for the preparation of this talk.

Outlay

- F_2 at Low and Intermediate Q^2

→ transition region with photoproduction $Q^2 \to 0$

→ F_2 in Next to Leading Order and DGLAP evolution

→ determination of F_L

→ extraction of $F_2^{c\bar{c}}$

→ measurements of the gluon density $xg(x, Q^2)$

- Jets

→ the gluon density from jets

→ jet shapes in DIS

→ measurement of α_S:

from integrated jet rates

from differential jet rates

from event shape variables

- Cross-Sections at High Q^2

→ influence of xF_3 and Z° exchange

→ Neutral Current cross-sections, high x

→ Charged Current cross-sections, W-mass

→ NC/CC ⇒ ratio u/d quark densities

Deep Inelastic Scattering at HERA

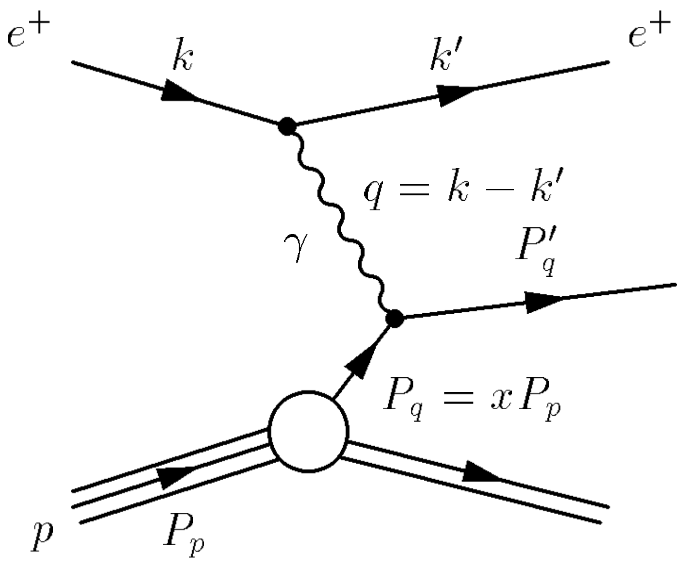

$Q^2 = -q^2 = -(k-k')^2$

4-momentum transfer

$x = Q^2/(2p\cdot q)$

parton momentum fraction

$y = p\cdot q/(p\cdot k)$

fractional energy transfer

$W^2 = (p+q)^2 \approx Q^2/x$

mass^2 of hadronic system

Structure Function F_2 in Quark Parton Model:

$$\frac{d^2\sigma^{e^\pm p}}{dx dQ^2} = \frac{2\pi\alpha^2}{Q^4 x}\,[1+(1-y)^2]\,F_2(x,Q^2)\,\cdot(1+\delta_{QED})$$

Related to the parton densities:

$$F_2(x) = x\sum_{i=1}^{n_f} e_i^2(q_i(x)+\overline{q}_i(x))$$

Longitudinal Structure Function: $F_L = 0$ in QPM

(Callan-Gross relation)

δ_{QED} : QED radiative corrections are precisely known ($\simeq 1\%$) and are corrected for

DIS Events at HERA

Low Q^2, low x event

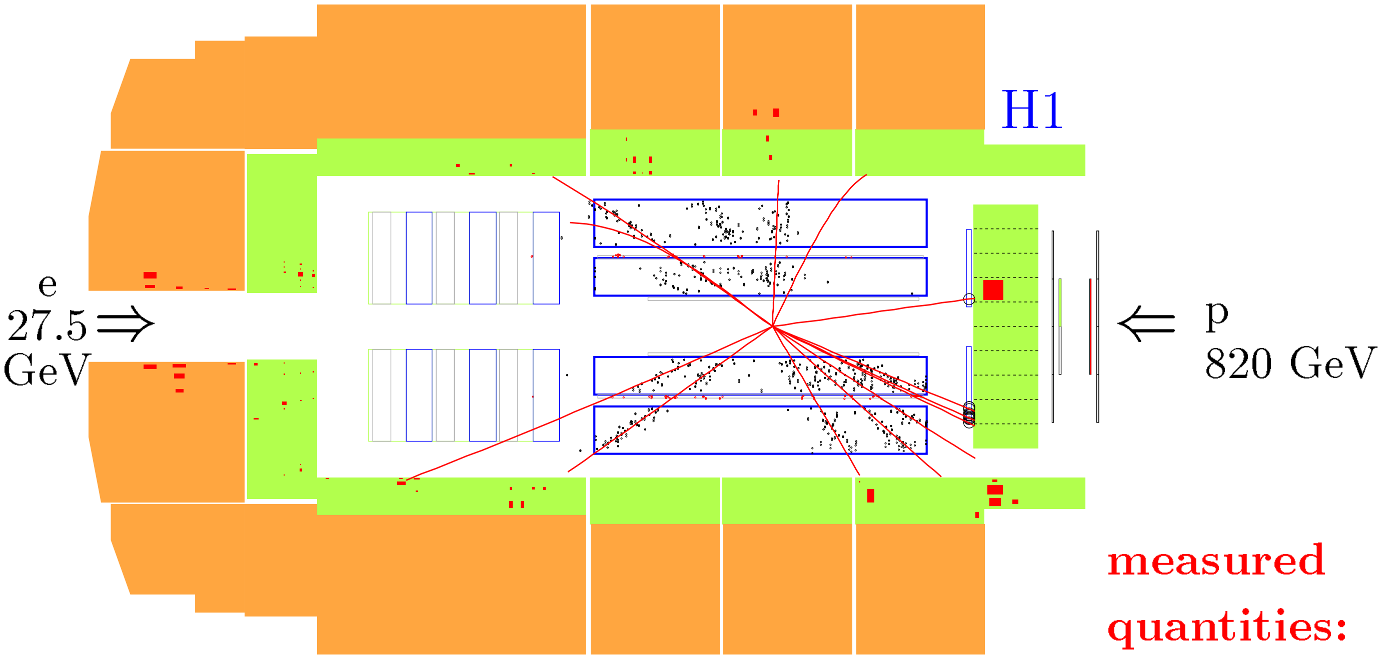

measured quantities:

e^+: energy E'_e

polar angle θ_e

hadrons: $\Sigma = \sum_i (E_i - p_{z,i})$

$p_{T,h} = \sum_i p_{T,i}$

$\tan \gamma_h/2 = \Sigma/p_{T,h}$

Di-jet event

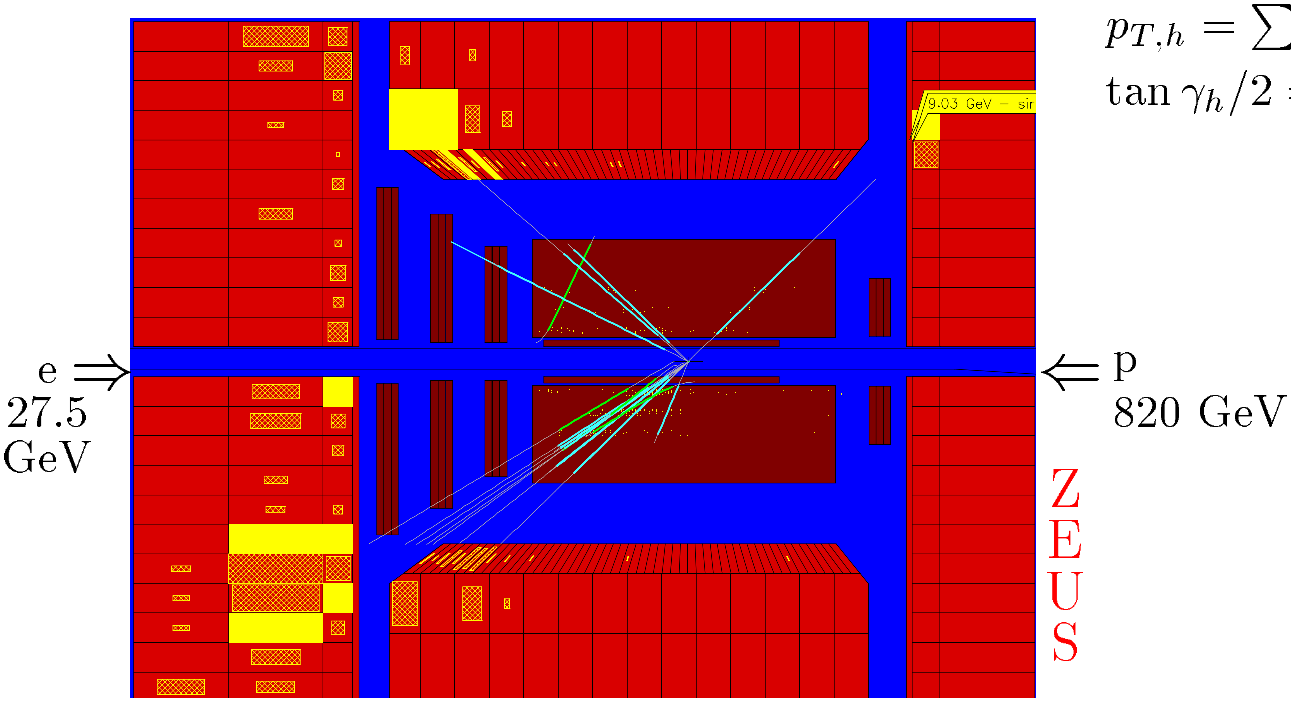

Kinematics and Measurement

Methods used for Kinematic Reconstruction:

- Electron Method: $y_e = 1 - \frac{E'_e}{E_e}\sin^2\frac{\theta_e}{2}$ $Q^2_e = 4E'_e E_e \cos^2\frac{\theta_e}{2}$
  most precise at low x but very sensitive to QED radiation
  poor x resolution at low y, but good Q^2 resolution in full range
- Σ Method: $y_\Sigma = \frac{\Sigma}{\Sigma + E'_e(1-\cos\theta_e)}$ $Q^2_\Sigma = \frac{E_e^2\sin^2\theta_e}{1-y_\Sigma}$
  good x resolution also at low y
  independent of QED initial state radiation
- $e\Sigma$ Method: $x_{e\Sigma} = x_\Sigma$ $Q^2_{e\Sigma} = Q^2_e$
  precise over the whole kinematic range
  ⇒ extension of the measurement at high x
- Double Angle Method: x_{DA}, Q^2_{DA} from θ_e, γ_h
  high precision at high Q^2, but sensitive to QED radiation
  independent of energy scale ⇒ used for calibration
- Hadron Method: $y_h = \frac{\Sigma}{2E_e}$ $Q^2_h = \frac{p^2_{T,h}}{1-y_h}$
  low precision, but only method for charged current

Measurement:

- (x, Q^2) binning: 5 bins/order of magnitude in x
  8 bins/order of magnitude in Q^2
- Purity and Stability of the (x, Q^2) bins $\geq 30\%$
- Background Subtraction (Photoproduction)
- Luminosity known within $1.5 - 2.5\%$ at HERA
- QED radiative corrections applied
  $\Rightarrow \left.\frac{d^2\sigma}{dx\,dQ^2}\right|_{Born}$ measured at fixed x, Q^2
  after bin center correction

$\boldsymbol{F_2}$ Results at HERA '94

1994: $\mathcal{L} \sim 3\ \mathrm{pb}^{-1}$

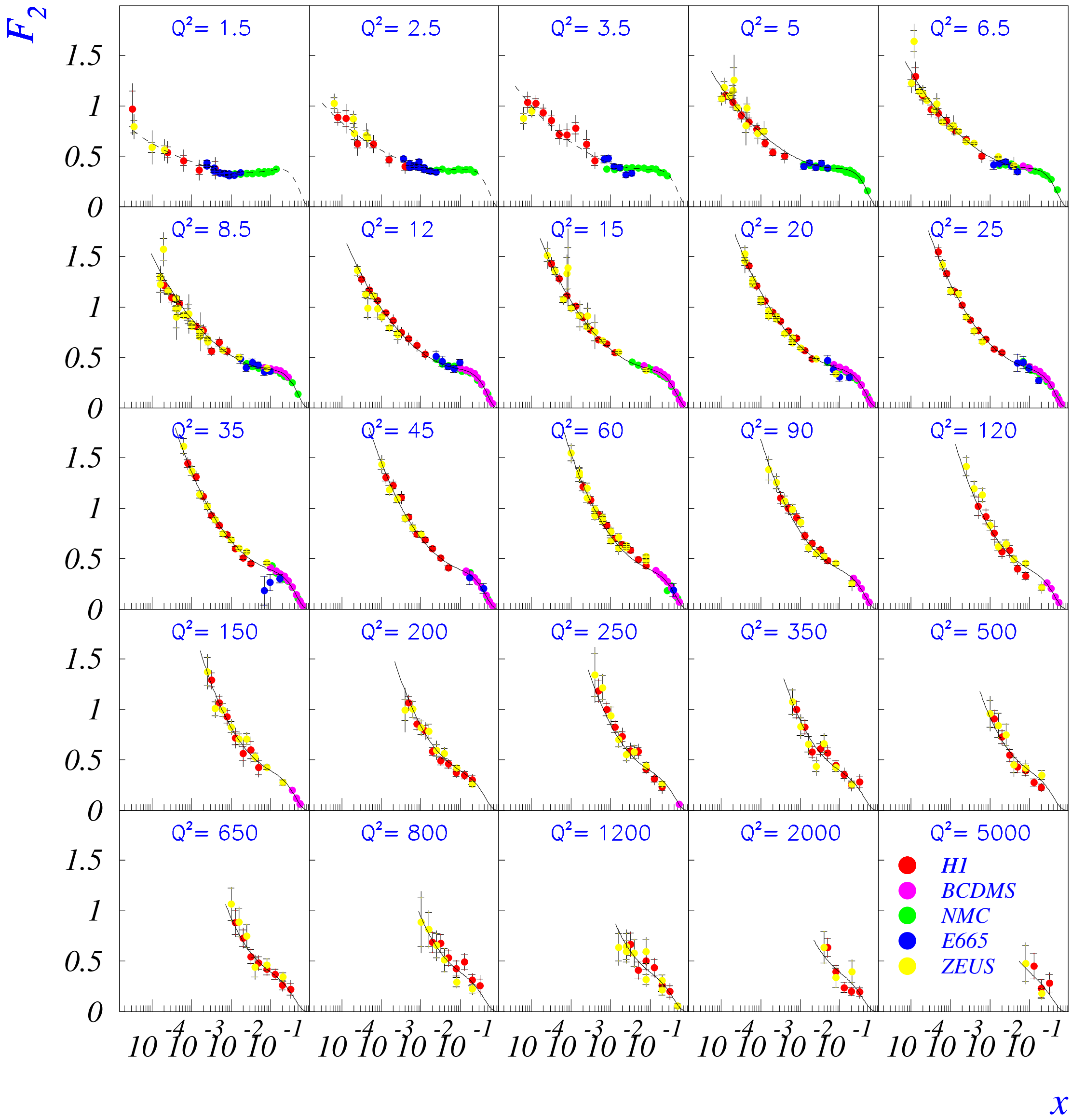

- Strong rise of $F_2(x, Q^2)$ at low x for a fixed Q^2
- Good agreement between HERA and fixed target exp.
- NLO QCD (DGLAP) fit gives good description down to $Q^2 = 1.5\ \mathrm{GeV}^2$
- Systematic errors $\sim 5\%$ dominant, except at high Q^2

Inclusive Measurements in $(\boldsymbol{x}, \boldsymbol{Q^2})$

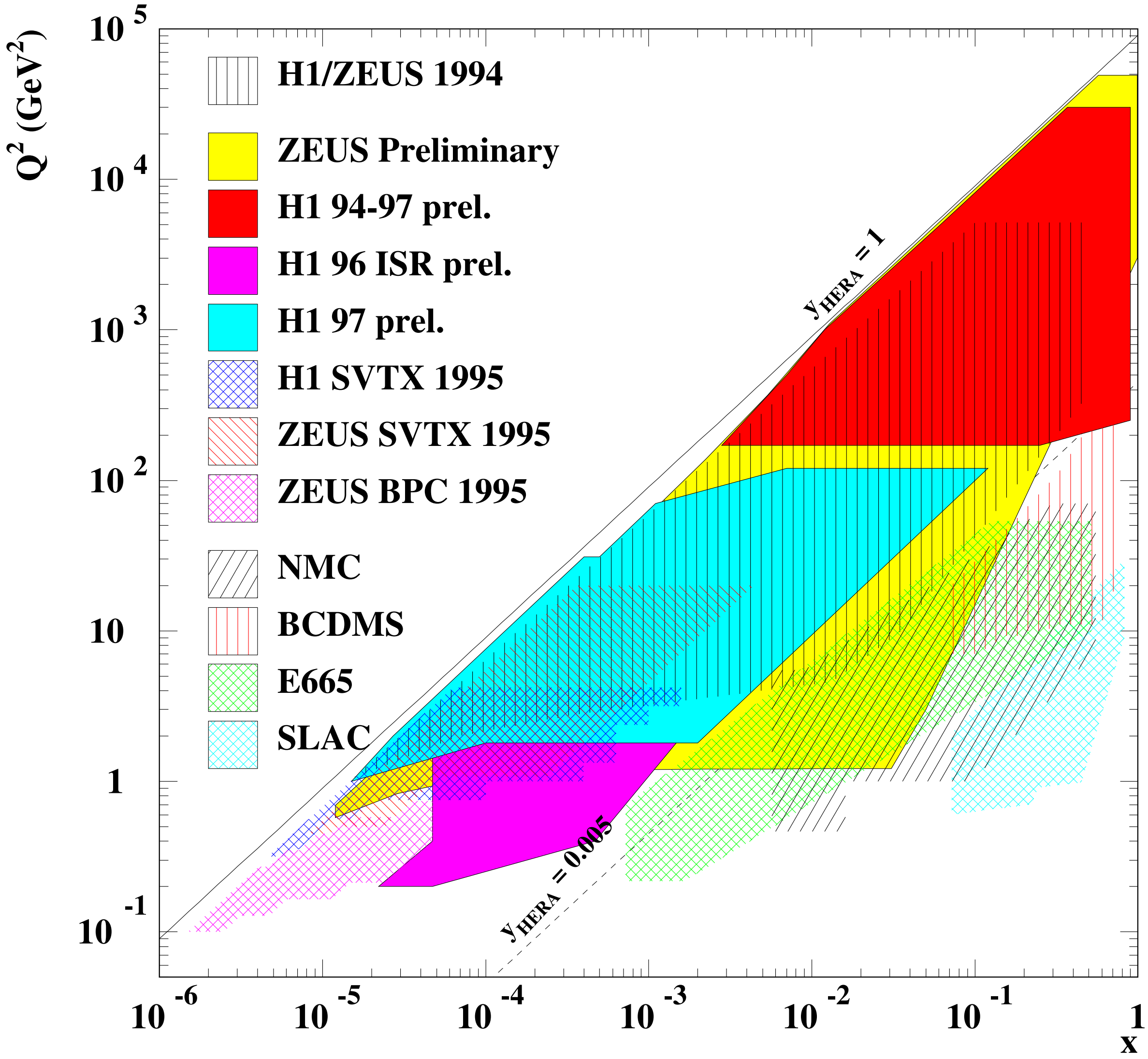

H1+ZEUS: Major extension of the kinematic range

- $x \to < 10^{-5}$: test low x limit of pQCD
- $x \to 0.65$: probe valence quark region
- $y \to 0.005$: overlap with fixed target experiments
- $y \to 0.82$: sensitivity to F_L
- $Q^2 \to 0.1$ GeV^2 : transition to γp
- $Q^2 \to 30000$ GeV^2: sensitivity to electro-weak effects

Access to the low Q^2 region

$$Q^2 = 4E'_e E_e \cos(\tfrac{\theta_e}{2})$$

1. shift of the interaction point $Q^2 \to 0.35\ \mathrm{GeV}^2$

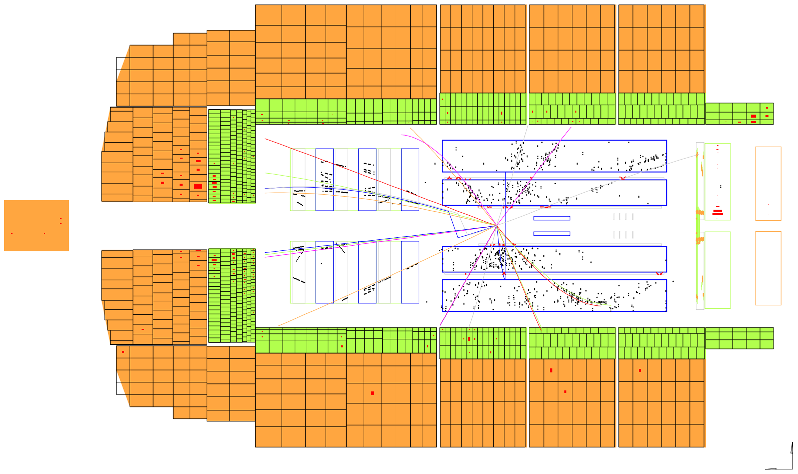

2. low angle detectors $Q^2 \to 0.1\ \mathrm{GeV}^2$

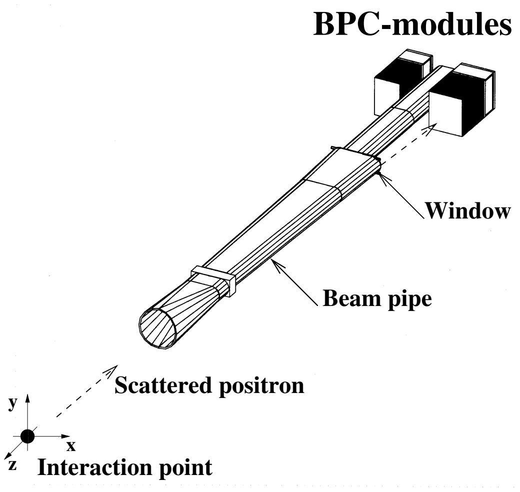

ZEUS: BPC (1995)
H1: VLQ (1998)

3. radiative events

$Q^2 \to 0.2\ \mathrm{GeV}^2$

higher x

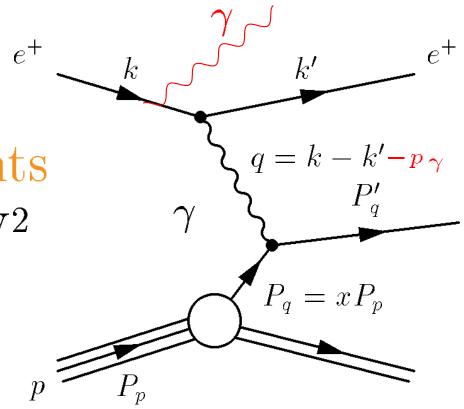

Cross-Sections at low $\boldsymbol{Q^2}$

Define total $\gamma^* p$ cross section:

$$\sigma_{tot}^{\gamma^* p}(W^2, Q^2) = \sigma_L^{\gamma^* p} + \sigma_T^{\gamma^* p} \simeq \frac{4\pi\alpha^2}{Q^2} F_2$$

$$W^2 \approx Q^2/x \quad \text{at low } x$$

$\Rightarrow$ comparison with γp data

- precise data from ZEUS and H1 on $\sigma^{\gamma p}$ ($Q^2 \approx 0$) and $\sigma^{\gamma^* p}$ at low Q^2 ($\approx 0.1 - 5$ GeV^2)
- 2 paradigms:
  - pQCD at very low Q_0^2 as in the GRV model, in which the DGLAP evolution starts with valence-like partons at $Q_0^2 \sim 0.4$ GeV^2
  - Regge approach as in the Donnachie-Landshoff model in which $\sigma_{tot} \propto W^{2\alpha_P}$, α_P is Q^2 independent and determined from hadron data ('soft Pomeron')
- interplay of pQCD ↔ Regge phenomenology ?

How does the transition take place?

Transition when $\boldsymbol{Q^2 \to 0}$

$\sigma_{\gamma^* p}(W, Q^2)$ at fixed W as function of Q^2:

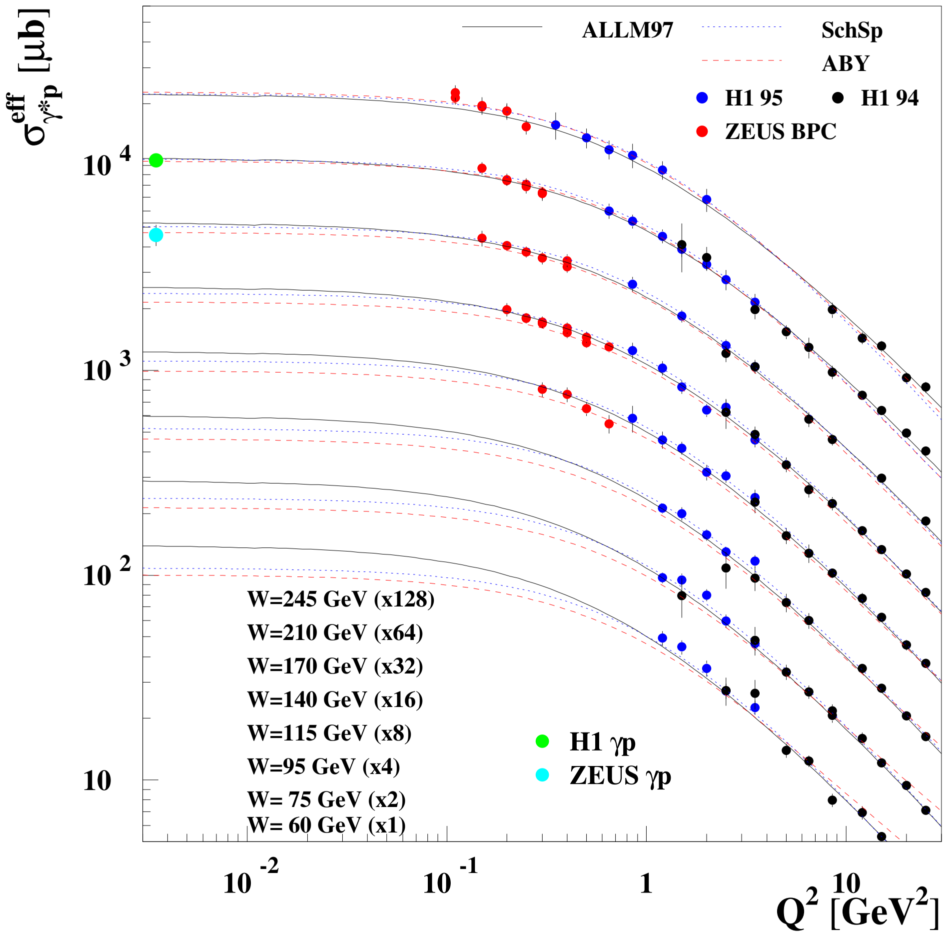

- Smooth transition to photoproduction $\sigma_{\gamma p}$ ● ●
- Constant Cross-Section up to $Q^2 \simeq 0.1$ GeV^2
- Change of behaviour $Q^2 \simeq 0.1 - 1$ GeV^2
- Fast decrease in the pert. QCD regime $Q^2 \gtrsim 1$ GeV^2
- ABY, SchSp and ALLM97 (all are fits to HERA data)
  $\Rightarrow$ good description in transition region,
  BUT no real theory
- New Measurements at $Q^2 \lesssim 0.1$ GeV^2 foreseen at HERA

Models for Transition DIS $\rightarrow \gamma$p

- at high Q^2 perturbative QCD (i.e. GRV model) describes the data
- at $Q^2 = 0$ the Regge approach (i.e. DL) is valid

How can we model the transition region ?

- Badelek and Kwiecinski (BK)
  ρ, ω, f from VDM plus
  pQCD above Q^2 matching value

- Schildknecht and Spiesberger (ScSp)
  Generalised VDM-model for
  $0<x<0.05$, $0<Q^2<350$ GeV^2 and $W>30$ GeV

- Capella et al (CKMT)
  Regge like, but with Q^2 dependent α_P
- Abramowicz et al (ALLM):
  Regge + QCD inspired parametrisation
  for all x and Q^2

- Adel, Barreiro and Yndurain (ABY)
  soft + hard input $a+bx^{-\lambda}$ at a low input scale
  each with its own NLO QCD evolution

Comparison to Photoproduction $Q^2 \approx 0$

Check the different models over the full W range in γp:

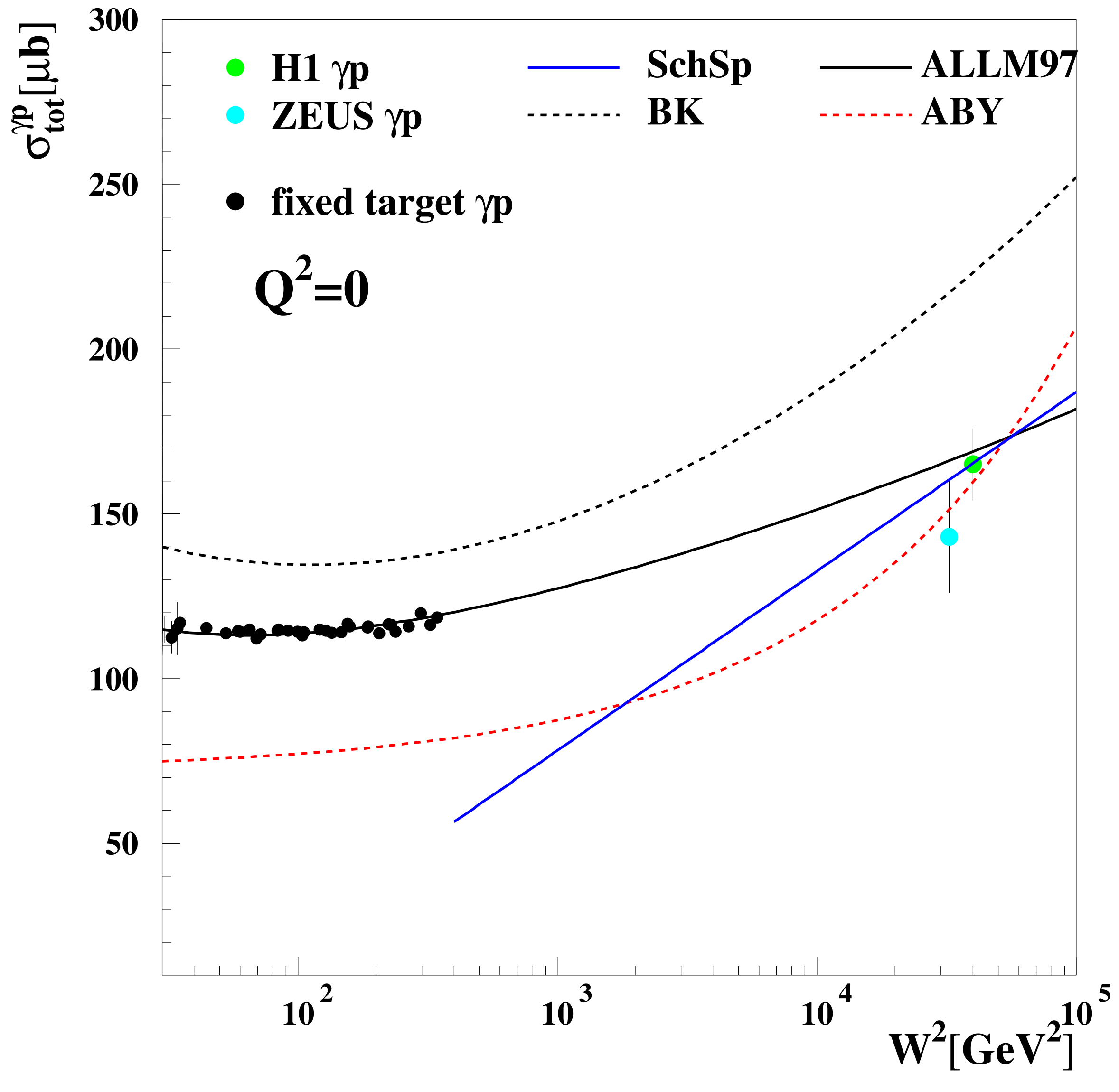

- only recent ALLM97 parametrization reproduces DIS and γp cross section over full W range
- ABY, SchSp and BK have wrong W dependence

Comparison to Photoproduction $Q^2 \approx 0$

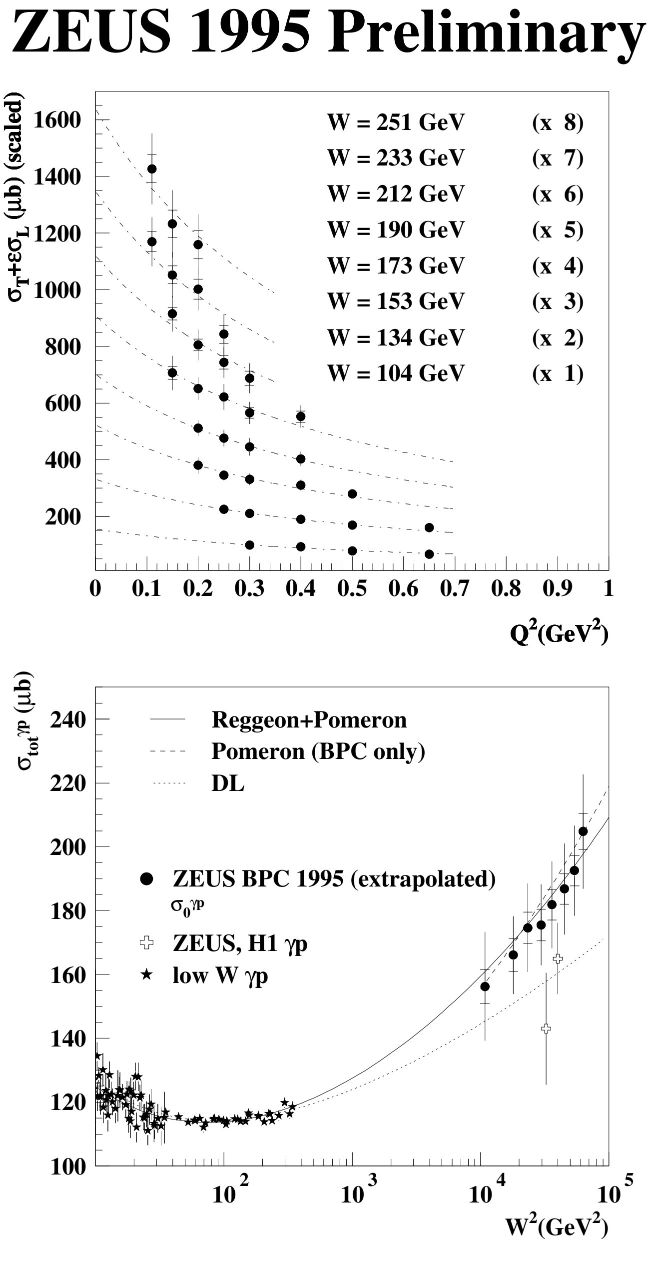

- a GVDM fit to the BPC data allows for the extrapolation of the BPC points at $Q^2 \simeq 0$
- a Regge fit (including Pomeron and Reggeon contributions) gives a good description of the extrapolated BPC data and of the low W real gamma-p data. The resulting α_P is 1.010 ± 0.002. The Hera gamma-p points are not well described by this fit.

$F_2(x, Q^2)$ at low Q^2

- F_2 still rises at $Q^2 = 0.11$ GeV^2 and x=6× 10^{-6}, but less strongly
- pQCD (i.e. GRV) describes the data at $Q^2 \gtrsim 1$ GeV^2

→ transition occurs at much lower Q^2 than expected

- DL Regge Model (Soft Pomeron) too low at low x, even at very low Q^2

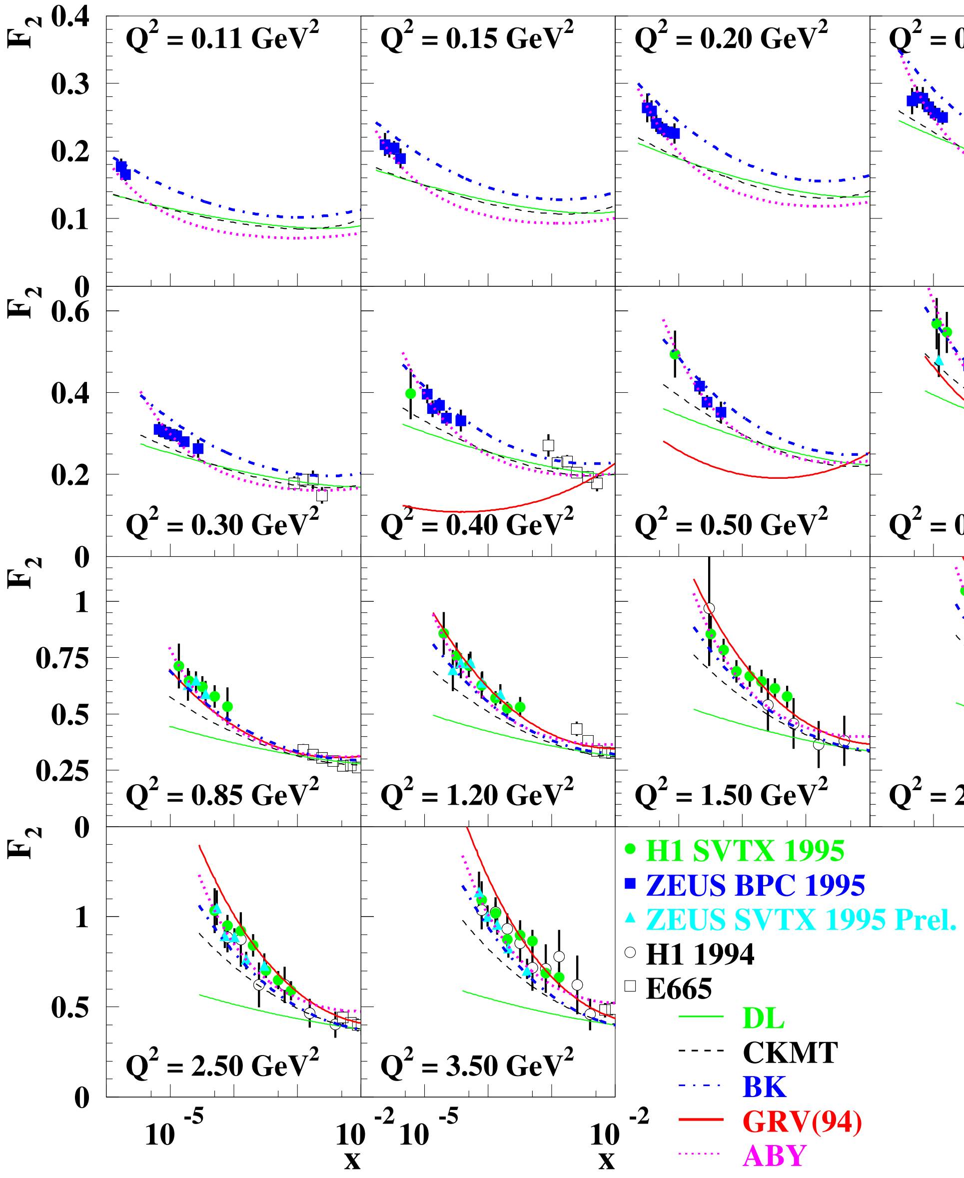

Transition Region: $\boldsymbol{x^{-\lambda}}$

Fit effective x slope at fixed Q^2 at low $x < 0.1$(H1) or 0.01(ZEUS)

$$\lambda \approx \frac{d\ln F_2}{d\ln 1/x} \qquad \text{i.e} \qquad F_2 \propto x^{-\lambda}$$

$\Rightarrow$ precision with H1 1997 data on $\lambda \simeq 1\%(\text{stat}) \oplus 5\%(\text{syst})$

How is λ decreasing towards $\lambda = 0.08$ as expected from Soft Pomeron at $Q^2 = 0$?

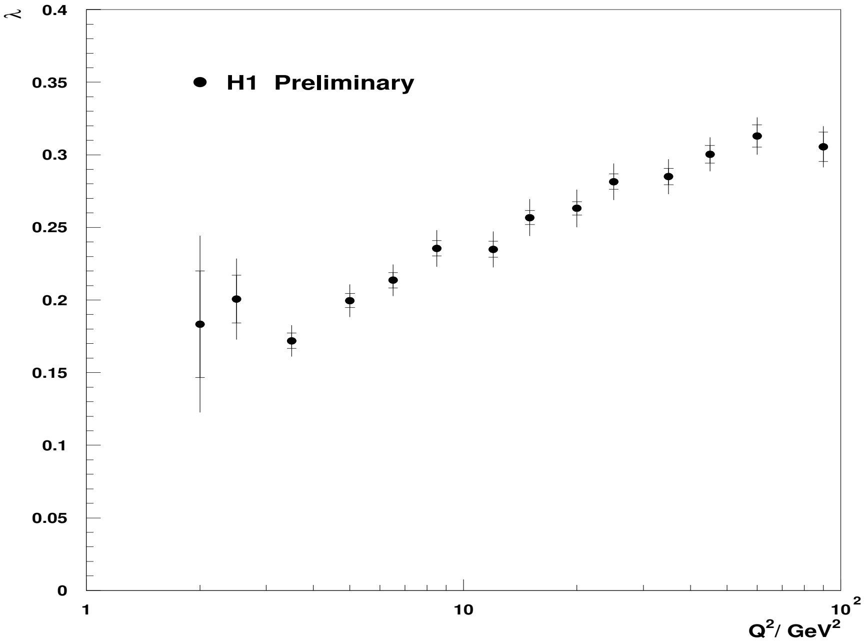

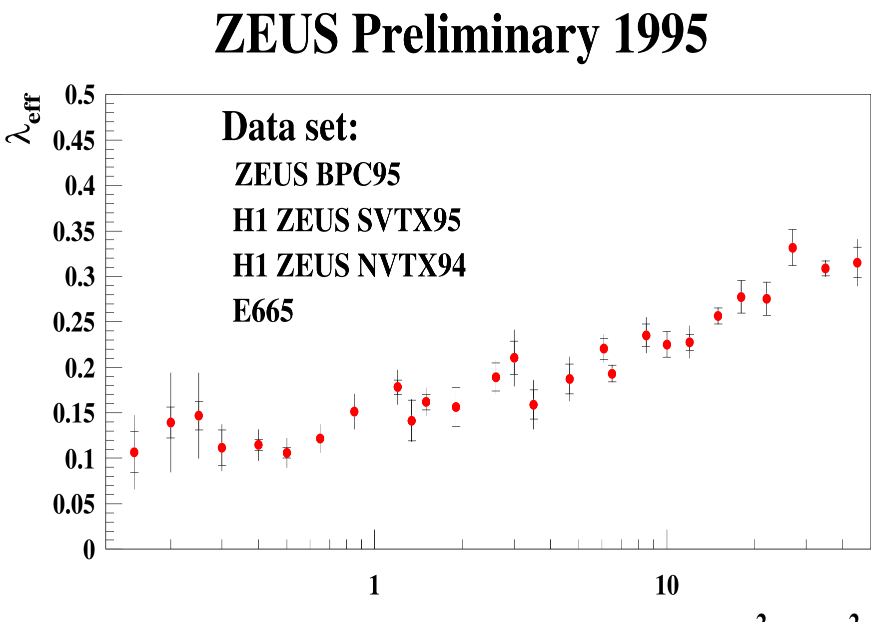

$\boldsymbol{F_2(x, Q^2)}$ at Intermediate $\boldsymbol{Q^2}$

- New high precision measurement with the data collected in 1996-97 by H1 and ZEUS ($\mathcal{L} \simeq 15$ pb^{-1}):

$$\left.\begin{array}{ll} \lesssim 1\% & \text{statistic} \\ \lesssim 4\% & \text{systematic} \end{array}\right\} \quad 2 \leq Q^2 \leq 100 \text{ GeV}^2$$

- Main error sources:
  - electron energy scale:

    $$\frac{\delta E_e}{E_e} = 0.5\% \qquad \text{based on the kinematic peak}$$

  - hadronic energy scale:

    $$\frac{\delta E_h}{E_h} = 3\% \qquad \text{based on } p_T \text{ balance } p_{T,h}/p_{T,e}$$

  - electron identification: $1 - 2\%$
  - background: $< 1\%$
  - radiative corrections: 1-2%
  - tracking efficencies: 1-2 %

→ slightly bigger errors at the edge of the phase space

Precision Measurement ⇒

Test of NLO perturbative QCD

$F_2(x, Q^2)$ vs Q^2 at low Q^2

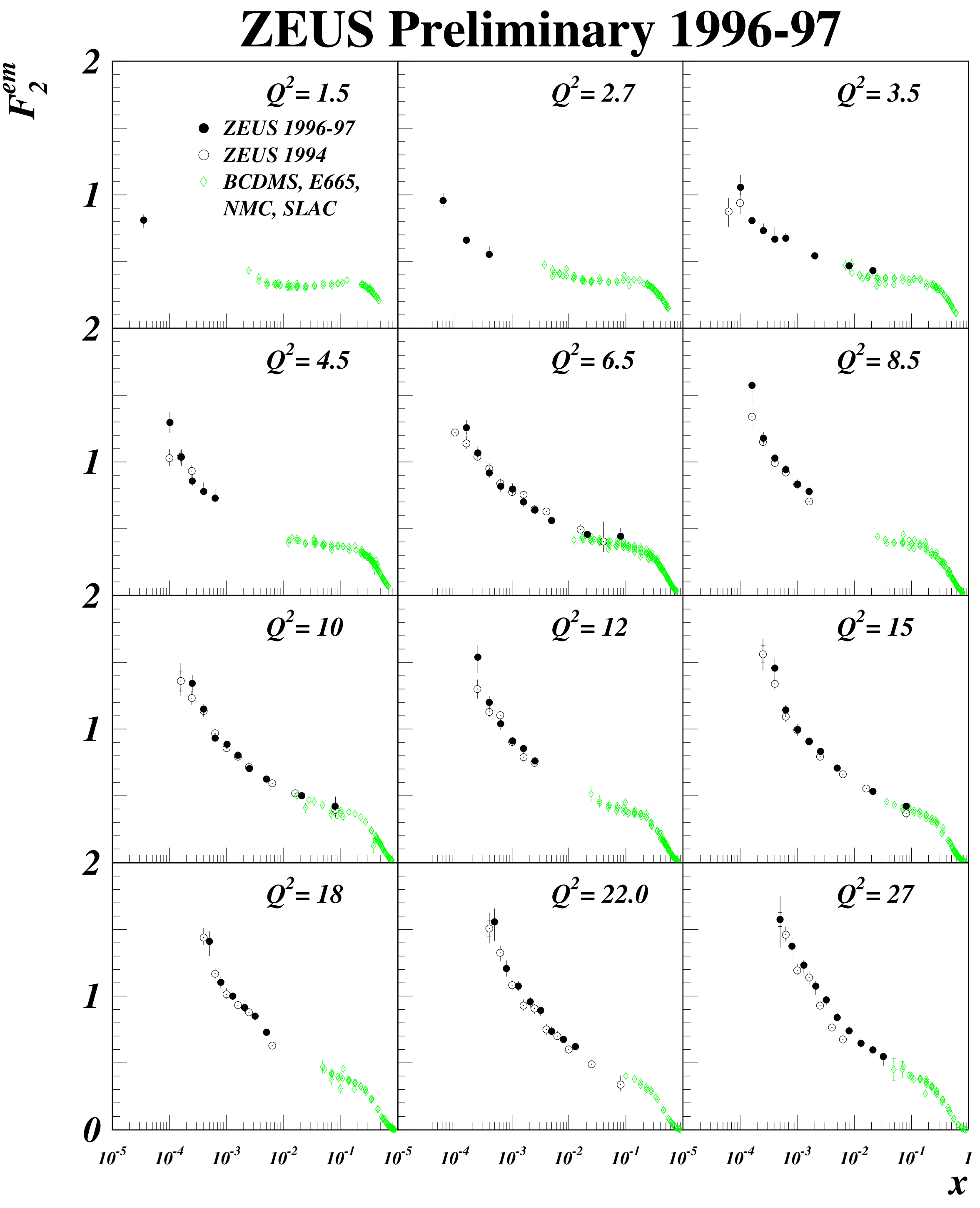

$F_2(x, Q^2)$ vs Q^2 at medium Q^2

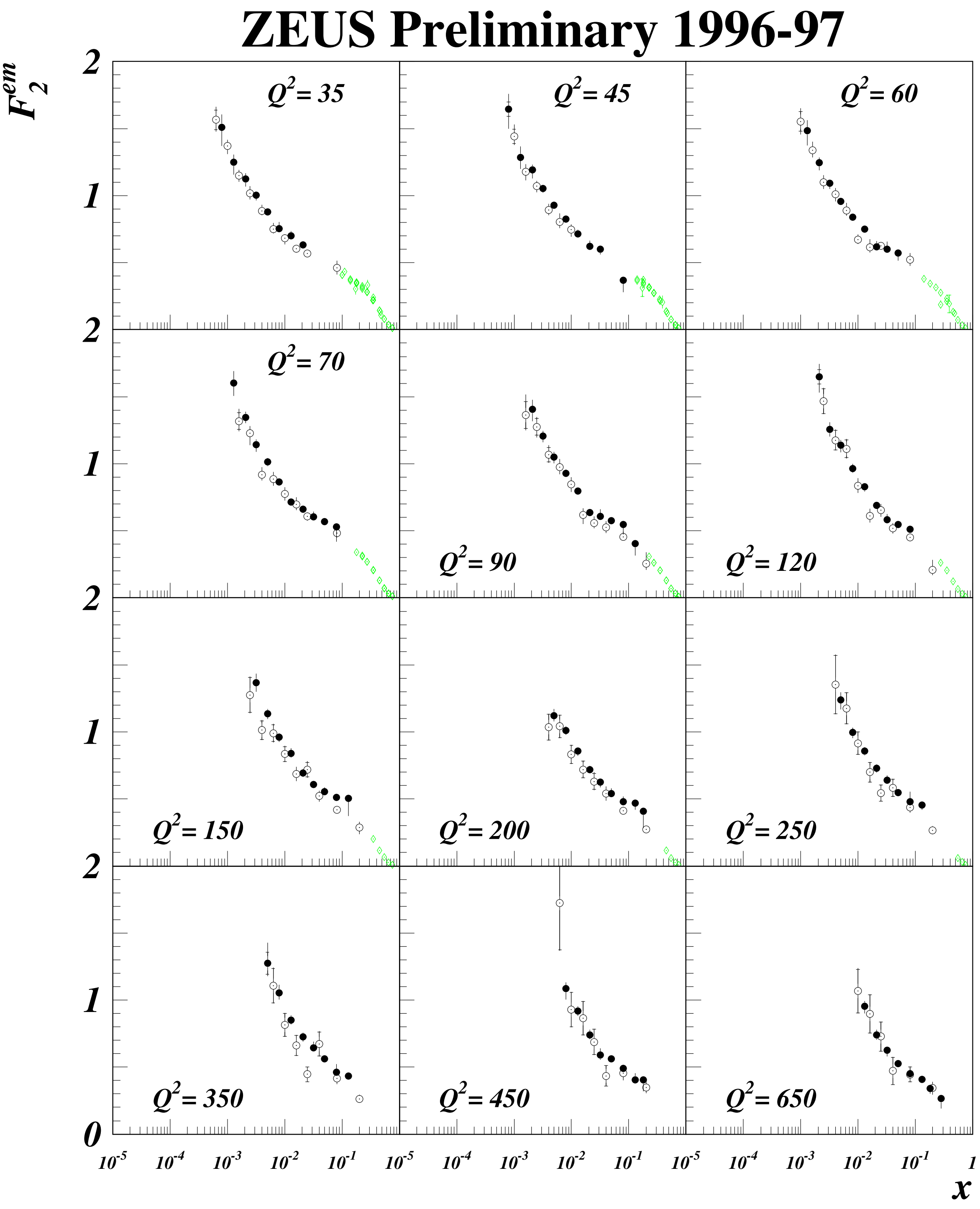

$F_2(x, Q^2)$ vs Q^2 at high Q^2

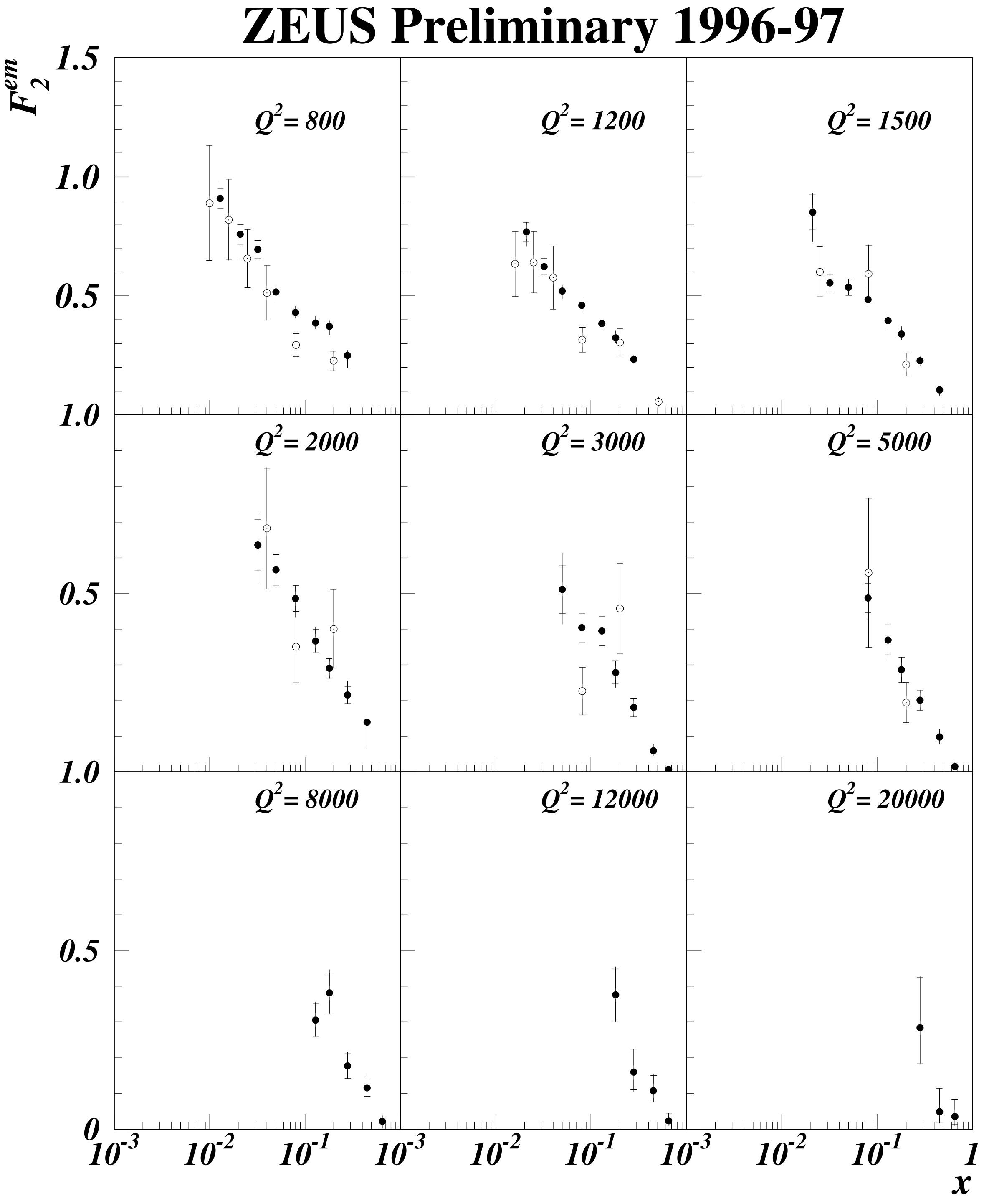
ZEUS Preliminary 1996-97

DGLAP Equations in QCD

- **From QCD (schematically):**

Leading Order: $F_2(x) = x \sum_{i=1}^{nf} e_i^2 (q_i + \bar{q}_i)$

NLO $\overline{\text{MS}}$: $F_2(x, Q^2) = x \sum_{i=1}^{n_f} e_i^2 C_q \otimes (q_i + \overline{q_i}) + C_g \otimes g$

- **Define parton densities:**

$xq_{NS} = \sum_{i=1}^{n_f} (xq_i - x\overline{q_i}) = xu_{val} + xd_{val}$ Non Singlet

$x\Sigma = \sum_{i=1}^{n_f} (xq_i + x\overline{q_i})$ Singlet

$xg(x)$ Gluon density

- **DGLAP evolution of parton densities:**

$$\frac{\partial}{\partial t} q_{NS}(x,t) = \frac{\alpha_s(t)}{2\pi} P_{qq}^{NS} \otimes q_{NS}(y,t); \quad t = \log \frac{Q^2}{\Lambda^2}$$

$$\frac{\partial}{\partial t} \begin{pmatrix} \Sigma(x,t) \\ g(x,t) \end{pmatrix} = \frac{\alpha_s(t)}{2\pi} \begin{pmatrix} P_{qq} & P_{qg} \\ P_{gq} & P_{gg} \end{pmatrix} \otimes \begin{pmatrix} \Sigma(y,t) \\ g(y,t) \end{pmatrix}$$

→ Splitting Functions P_{ij} known to NLO
→ Coefficient Functions $C_{q,g}$ known to NLO

⇒ DGLAP predicts Q^2 slope of $F_2(x, Q^2)$
for given parton densities at $Q^2 = Q_0^2$

No prediction on the x dependence at Q_0^2
⇒ must be obtained from a QCD fit to the data

H1 and ZEUS NLO-QCD fits

- Fit Conditions and Assumptions:

- u,d,s massless partons
- c from BGF calculated at NLO (Riemersma et al.) in $\overline{MS}$ $m_c = 1.5$ GeV, scale $\mu^2 = Q^2 + m_c^2$
- Full treatement of correlated systematic errors
- Theoretical uncertainties from α_s and m_c
- Momentum Sum rule: $\int_0^1 dx\, x(g + \Sigma) = 1$
- Quark Counting Rules: $\int_0^1 dx\, u_v = 2$, $\int_0^1 dx\, d_v = 1$
- Assume $\bar{u} = \bar{d}$ s= 20% of total sea at Q_0^2
- Discard data with x > 0.5 at low Q^2

- Input Parametrisations:

$$xg\ (x, Q_0^2) = A_g x^{B_g} (1-x)^{C_g} (1 + D_g x)$$
$$xu_v(x, Q_0^2) = A_u x^{B_u} (1-x)^{C_u} (1 + D_u x + E_u \sqrt{x})$$
$$xd_v(x, Q_0^2) = A_d x^{B_d} (1-x)^{C_d} (1 + D_d x + E_d \sqrt{x})$$
$$xS\ (x, Q_0^2) = A_s x^{B_s} (1-x)^{C_s} (1 + D_s x + E_s \sqrt{x})$$

- Datasets Used:
  - ZEUS: ZEUS 94+95 data with $Q^2 > 1$ GeV^2
    - NMC and BCDMS p+d data
    - $Q_0^2 = 7$ GeV^2
    - $\alpha_s(M_Z^2)$=0.118
  - H1: H1 94+95+96+97 data with $Q^2 > 2$ GeV^2
    - NMC and BCDMS p+d data
    - $Q_0^2 = 2$ GeV^2
    - $\alpha_s(M_Z^2) = 0.118\pm 0.05$
    - $D_g = 0$

F_2 and perturbative QCD

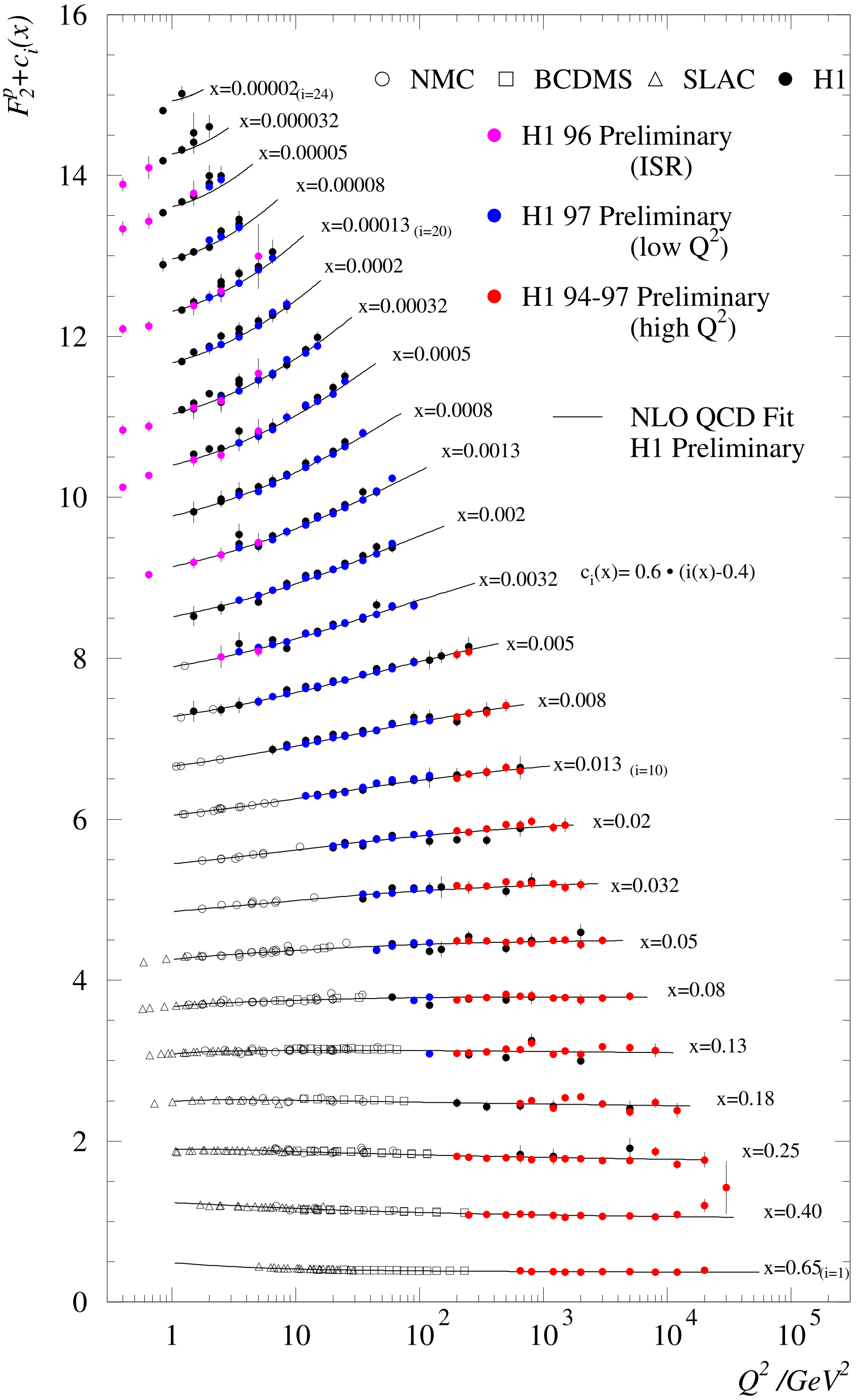

- Good description of the data by the NLO DGLAP fit over more than 4 orders of magnitude in x and Q^2

$F_2(x, Q^2)$ vs NLO QCD fit

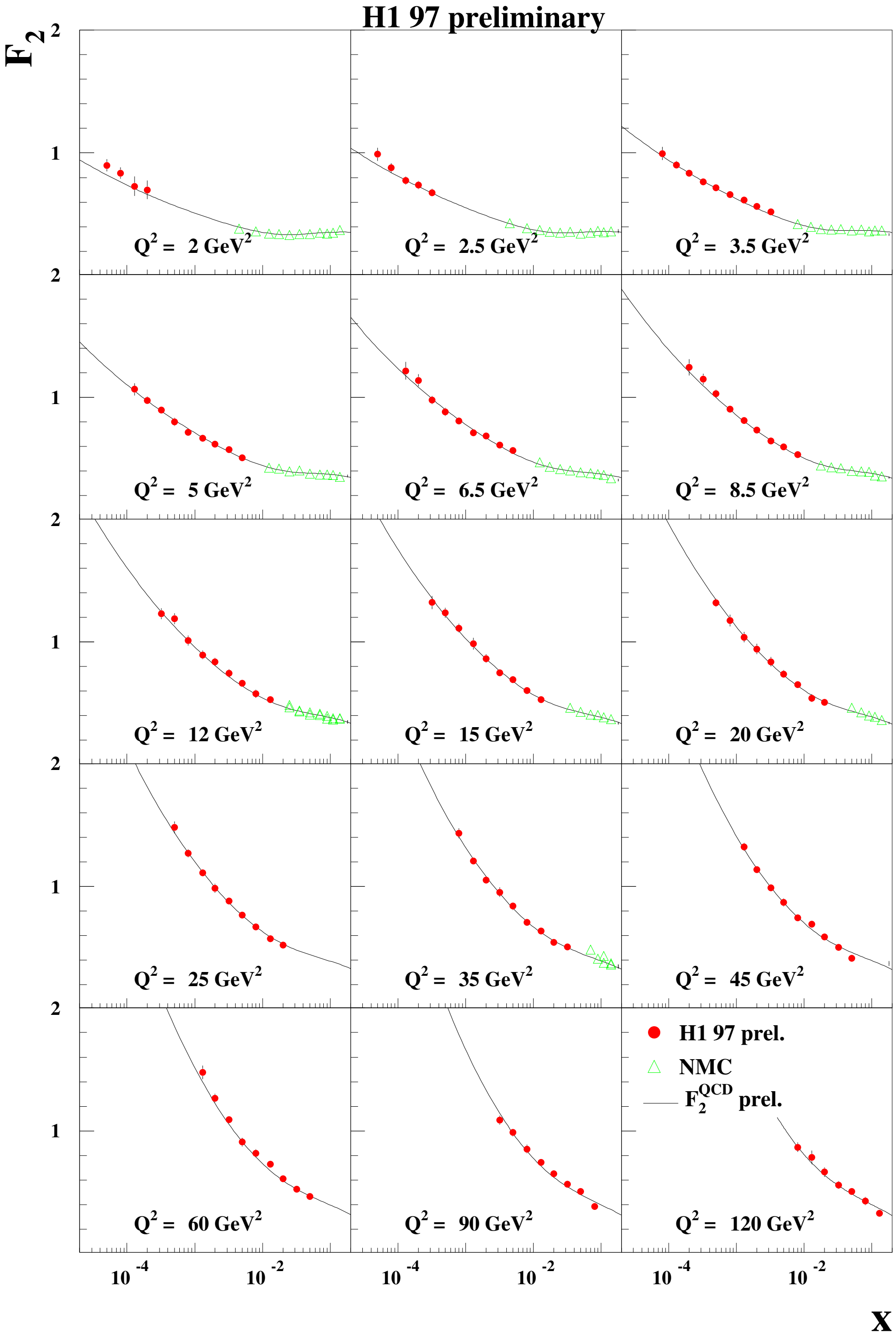

- F_L assumption based on QCD fit (small influence)
- Precision: $\simeq 1\%$ (stat) 3-4 % (syst)
- DGLAP describes the data very well...

  ...even at low Q^2 and low x!

Scaling Violations at Low $\boldsymbol{x}$

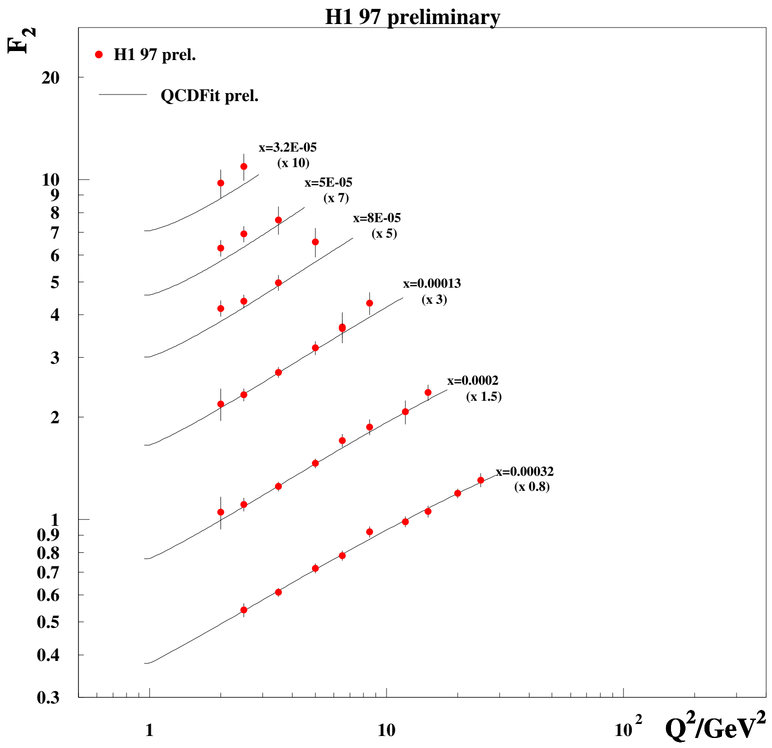

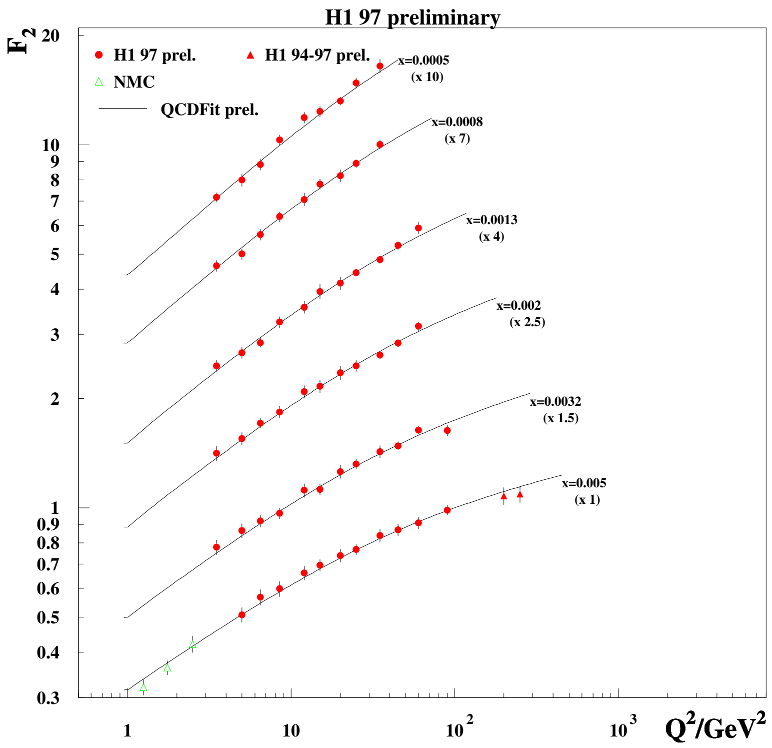

- Large slope $\mathrm{d}F_2/\mathrm{d}\ln Q^2$ at low x which stops increasing at $x \simeq 10^{-4}$
- Scaling violations due to large gluon radiation at low x

Towards Scaling at $\boldsymbol{x} \simeq 0.1$

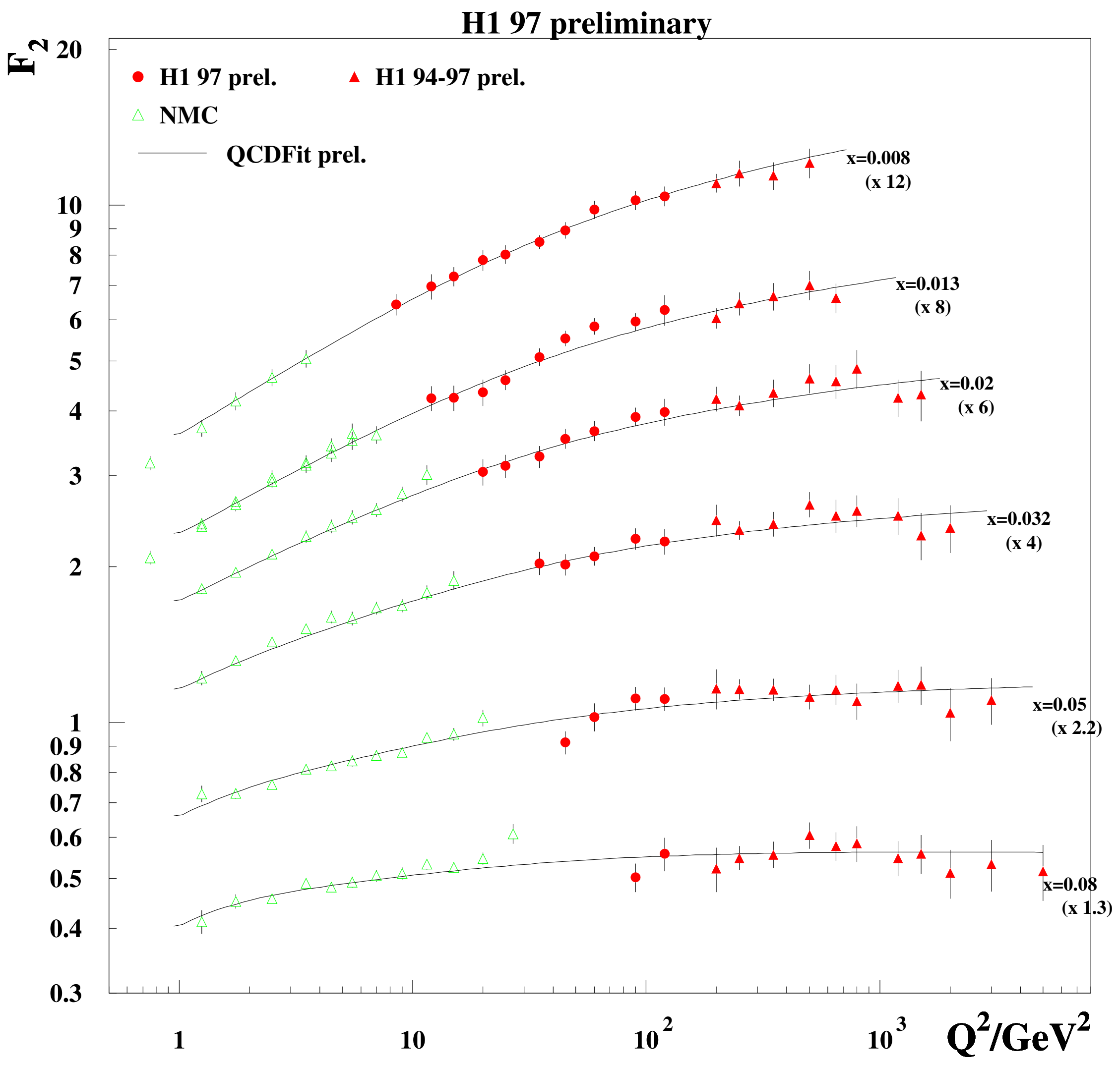

- Precision on F_2 at HERA now comparable to fixed target experiments (few %)
- Good agreement between the measurements of the fixed target experiments and HERA
- Scaling at $x \approx 0.1$ observed up to 5000 GeV^2

Scaling Violations at High $\boldsymbol{x}$

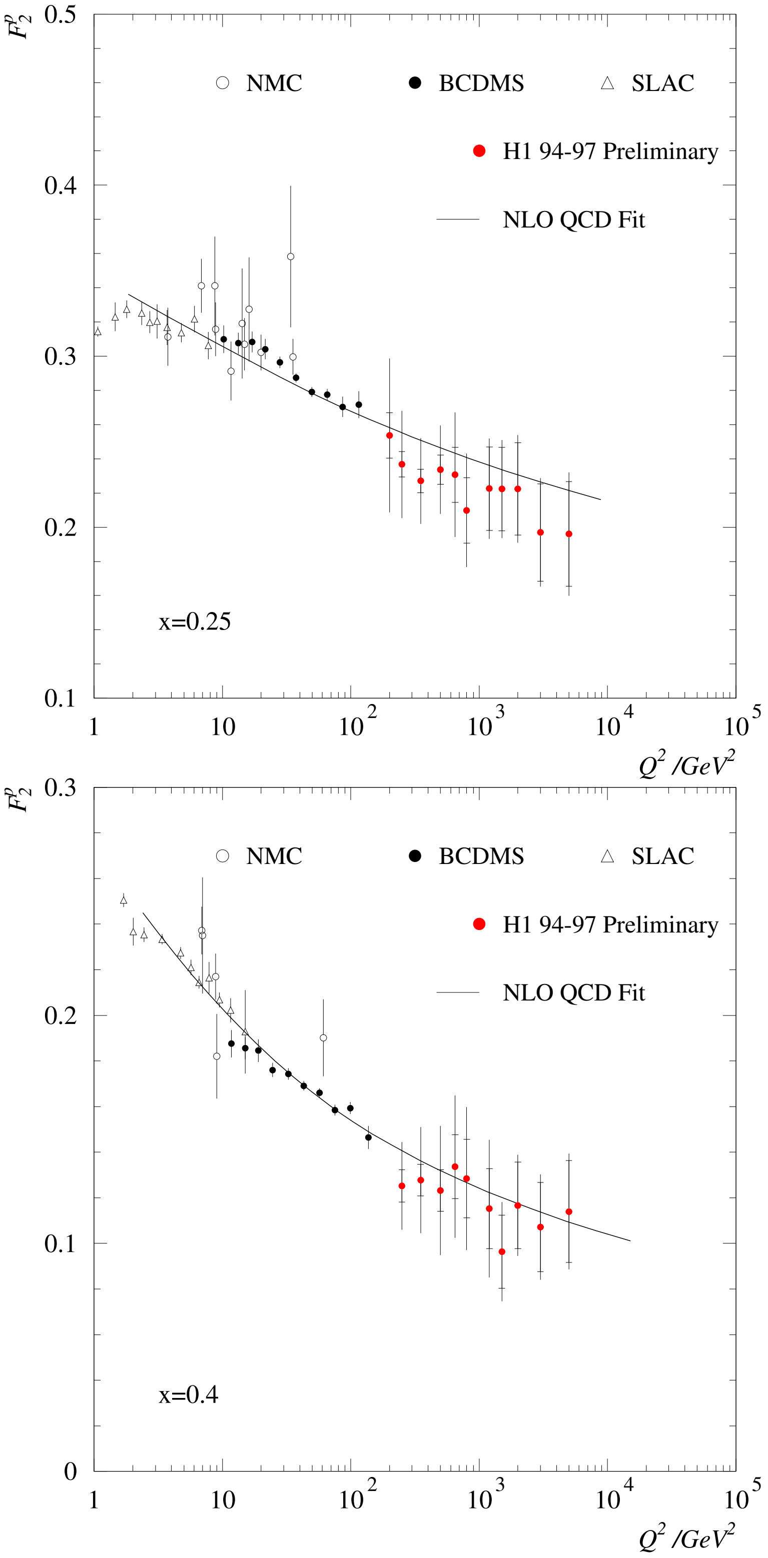

- Still large statistical error at high x, which is reachable at HERA only at $Q^2 \gtrsim 100$ GeV^2
- Good description of the data by NLO DGLAP fit.

Extraction of $\boldsymbol{F_L}$ from Cross-Sections

Reduced x-section: $\sigma_{red} = \frac{1}{\kappa}\frac{d^2\sigma}{dxdQ^2} = F_2 - \frac{y^2}{Y_+}F_L$

with $\kappa = \frac{2\pi\alpha^2 Y_+}{Q^4 x}$ and $Y_+ = 1 + (1-y)^2$

⇒ subtract at high y: $F_L = \frac{Y_+}{y^2}\left(F_2^{fit} - \frac{1}{\kappa}\frac{d^2\sigma^{exp}}{dxdQ^2}\right)$

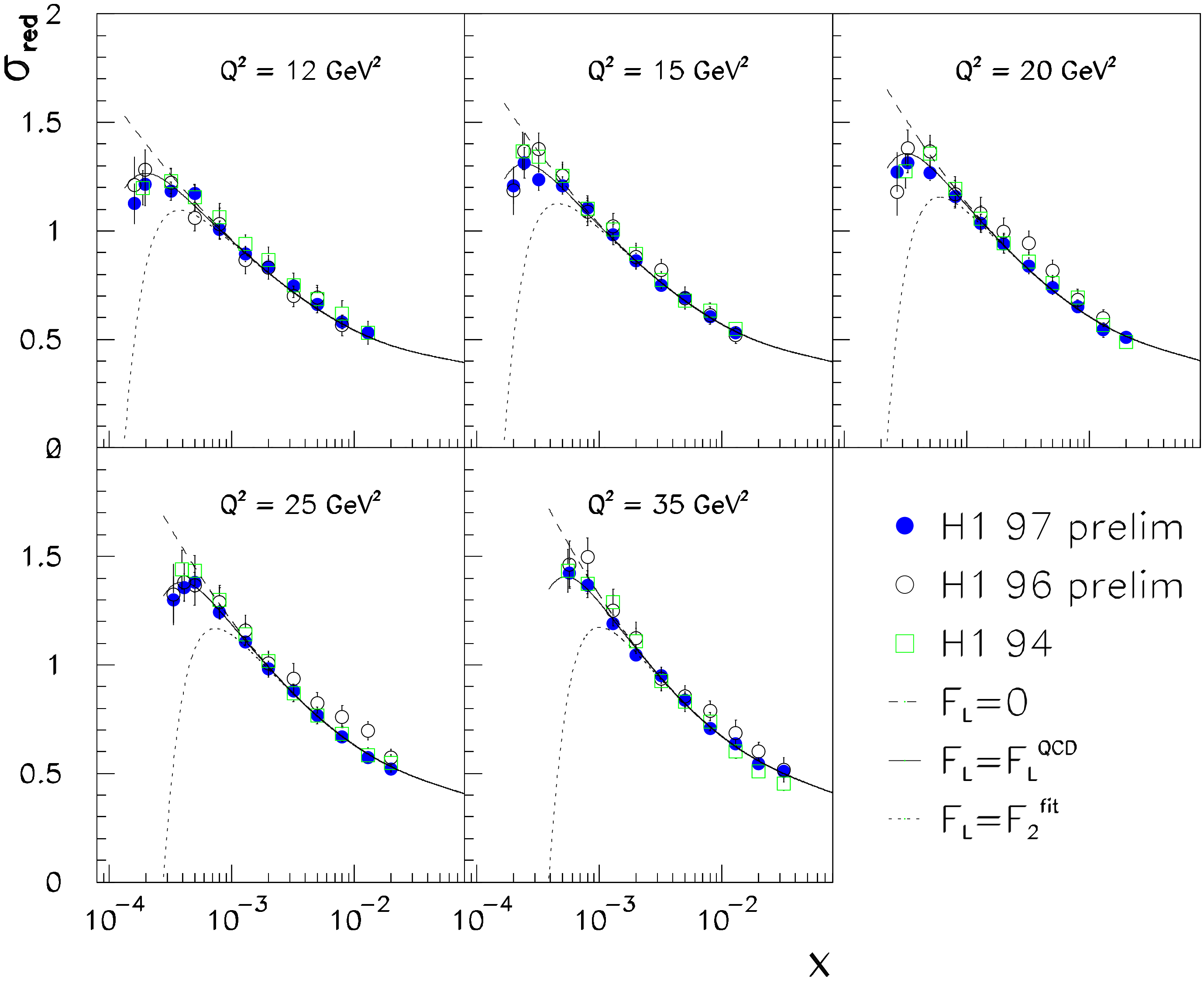

DGLAP NLO QCD fit to F_2 (H1-94..97, $y < 0.35$)

$\partial\sigma/\partial \ln y$: sensitive to F_L

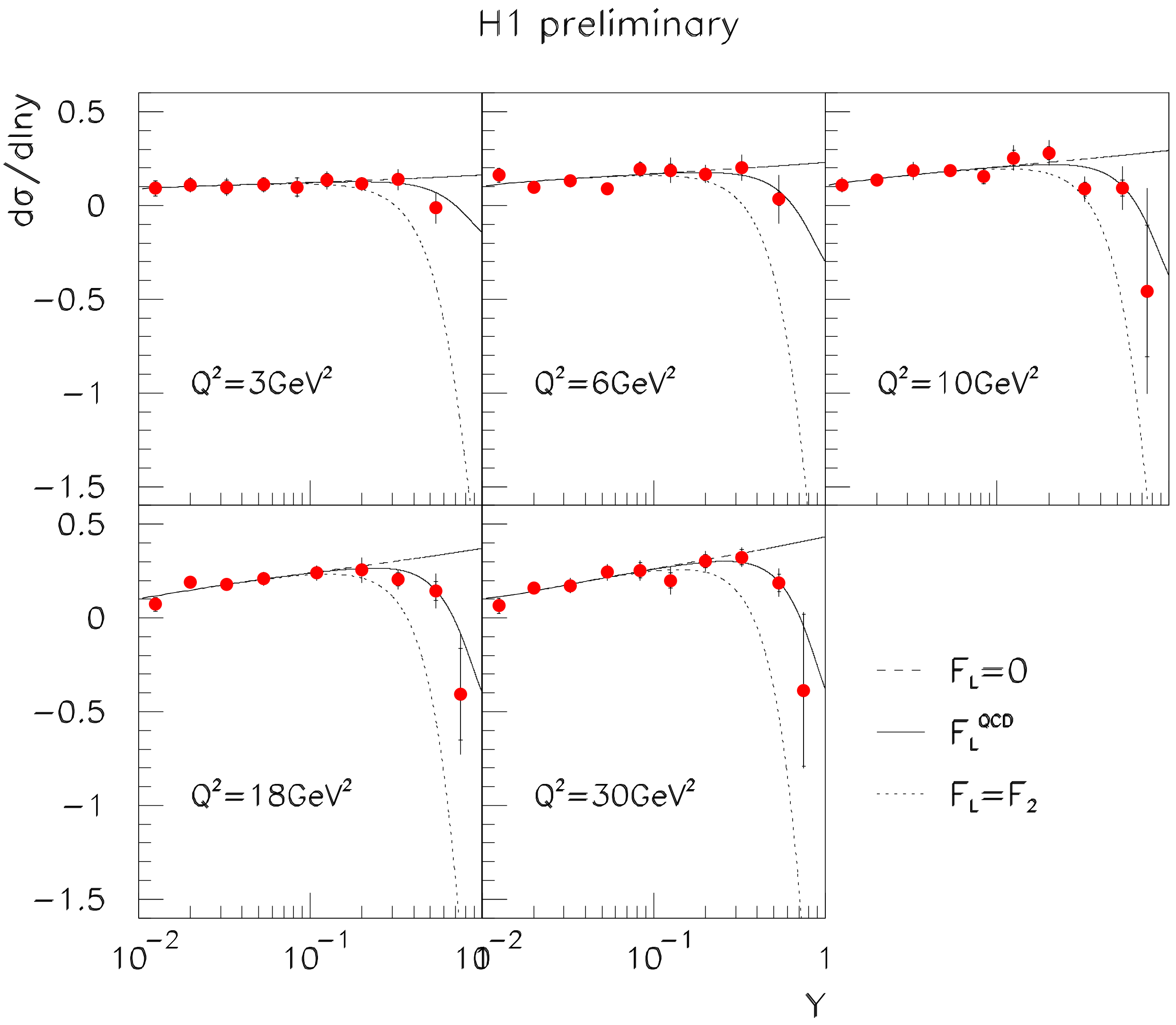

at fixed Q^2, the derivative of the reduced cross-section is: σ:

$$\frac{\partial\sigma}{\partial \ln y} = -\frac{\partial F_2}{\partial \ln x} - F_L \cdot 2y^2 \cdot \frac{2-y}{Y_+^2} + \frac{\partial F_L}{\partial \ln x} \cdot \frac{y^2}{Y_+}$$

- assume $\partial F_2/\partial \ln y = A \ln y + \mathrm{B}$
- Straight line fit to $\partial\sigma/\partial \ln y$ in Q^2 bins at $y < 0.2$

(This approximation has been checked with the QCD fit)

$\Rightarrow$ Access to lower Q^2 than with subtraction method
(No QCD extrapolation at low x, low Q^2)

Determination of the Longitudinal s.f. $\boldsymbol{F_L}$

Two methods used for the F_L determination:
The subtraction method (●) and the derivative method(⋆)

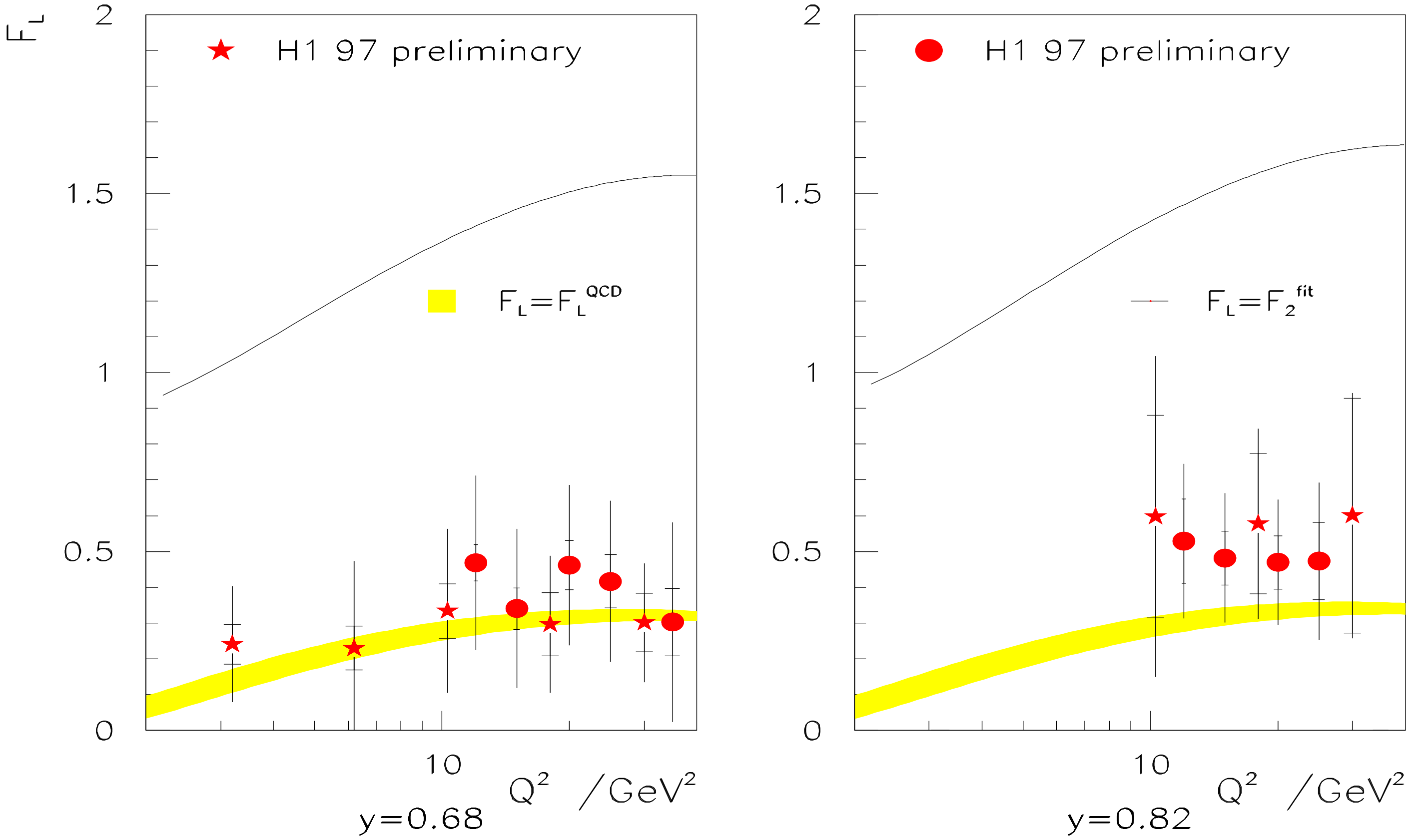

- Extracted F_L compatible with QCD prediction
- Good agreement between the two extraction methods, which use the same data but different characteristics of the F_2 and F_L behaviour.
- Slight tendency of $F_L^{H1} > F_L^{QCD}$ at the highest y

Note: the systematic errors of the points at the same y are correlated

Future: Measure F_L Directly by Changing Beam Energies

The Charm Contribution to $\boldsymbol{F_2}$

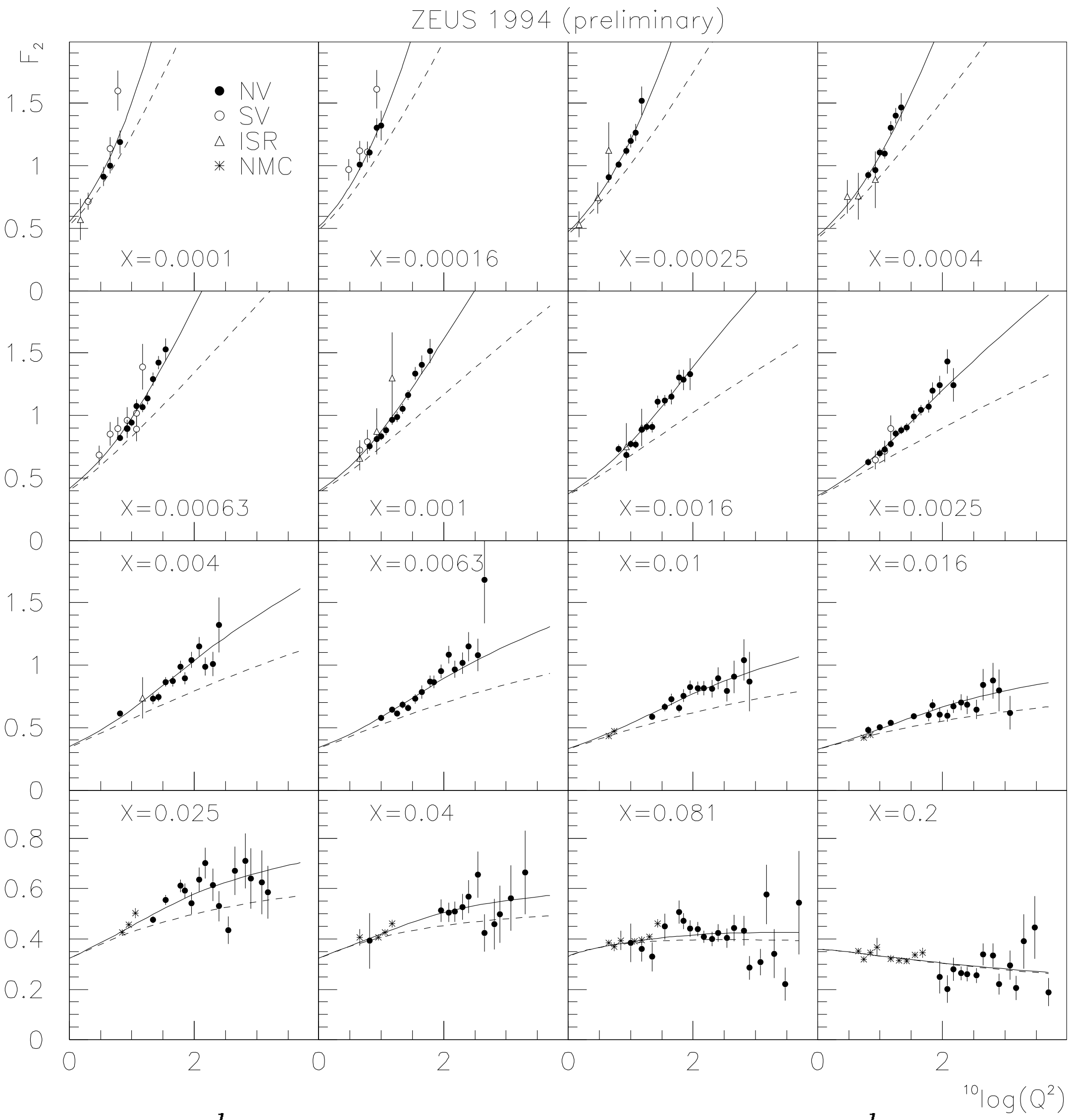

$$— = F_2^{u,d,s} + F_2^c = F_2 \qquad - - - = F_2^{u,d,s}$$

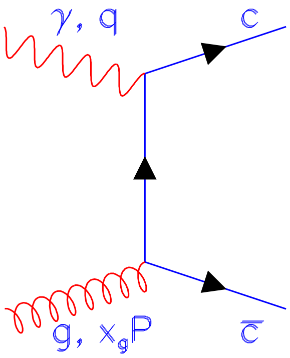

- F_2^c from Boson-Gluon-Fusion generated dynamically m_c taken into account
- charm contribution up to ~ 25 %

F_2^c can be estimated with the QCD fitCan we

Charm in DIS

Select in DIS sample ($1 < Q^2 < 600$ GeV^2, $0.02 < y < 0.7$)

$D^{*+} \rightarrow D^0\pi^+ \rightarrow (K^-\pi^+)\pi^+ + c.c., with$

$M(K\pi)$: 1.80 – 1.92 GeV ; $M(K\pi\pi) - M(K\pi)$: 143 – 148 Me

$1.5 < p_T(D^*) < 15$ GeV,

$$\Rightarrow \sigma(ep \rightarrow eD^*X) = 8.55 \pm 0.40^{+0.30}_{-0.24}\ \text{nb}$$

ZEUS PRELIMINARY 96-97

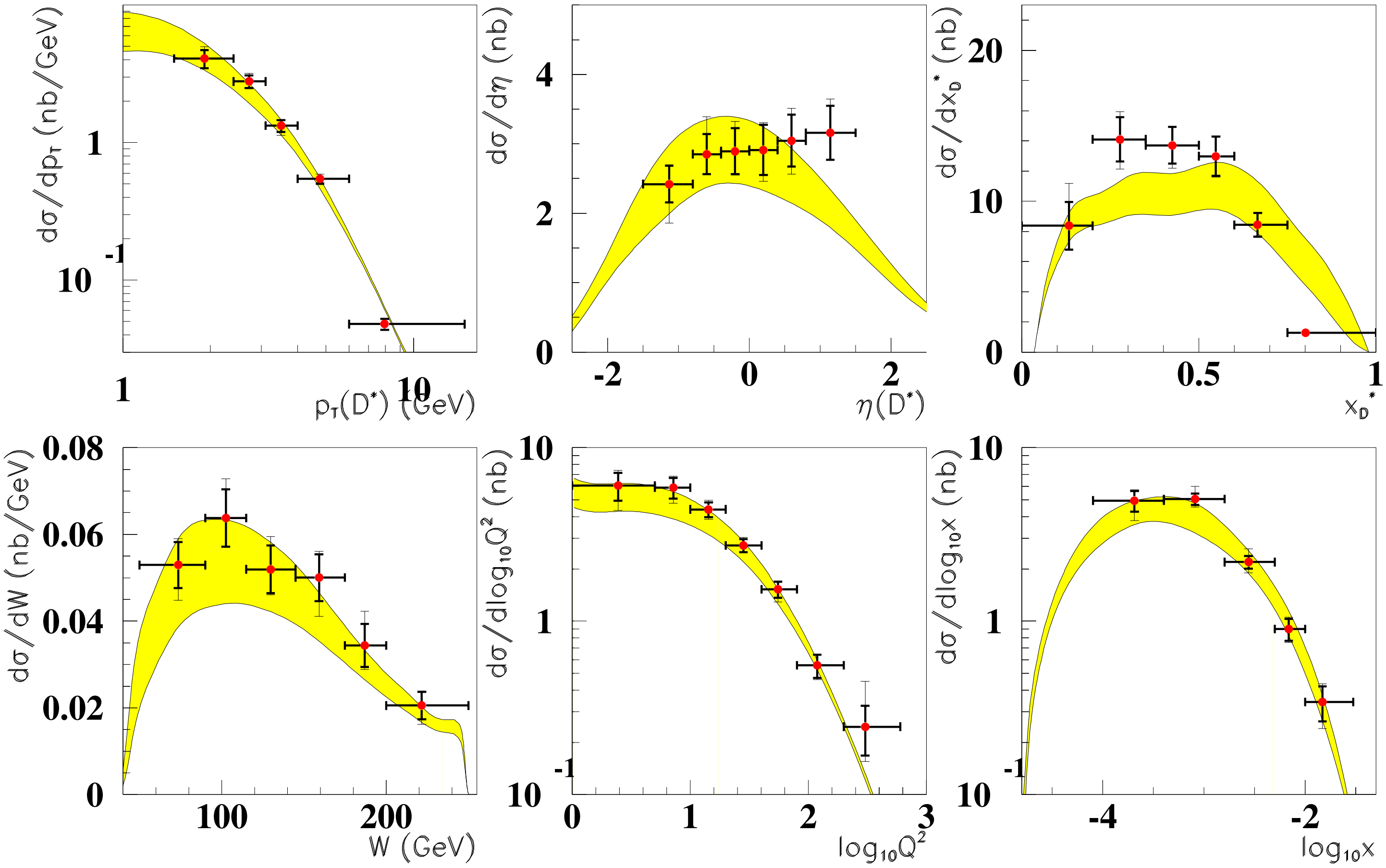

$\Rightarrow$ agreement with “massive” NLO pQCD calculation except

high-η ? **low-$x(D^*)$?**

Measurement of $\boldsymbol{F_2^c}$

$$\frac{d^2\sigma_{c\bar{c}X}}{dx\,dQ^2} = \frac{2\pi\alpha^2}{xQ^4}[1+(1-y)^2]F_2^c(x,Q^2)$$

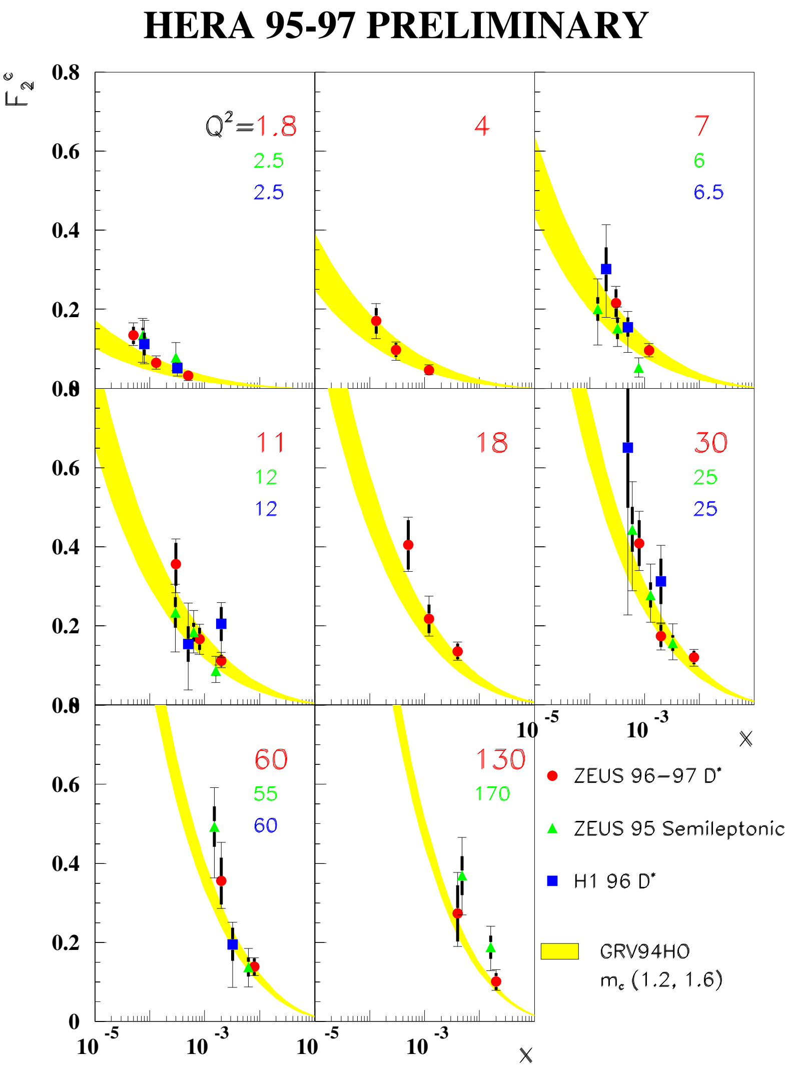

Extraction of F_2^c requires:

- extrapolation to full $\{\eta, p_T\}$ range.
- fragmentation functions $c \rightarrow D$.
- F_L^c is small and neglected.

- Precision $\simeq 15-20\%$
- Significantly more precise than earlier measurements
- Steep rise towards small $x \rightarrow$ gluons
- Good agreement between direct measurement and indirect prediction from perturbative QCD

The Gluon Density from the Charm

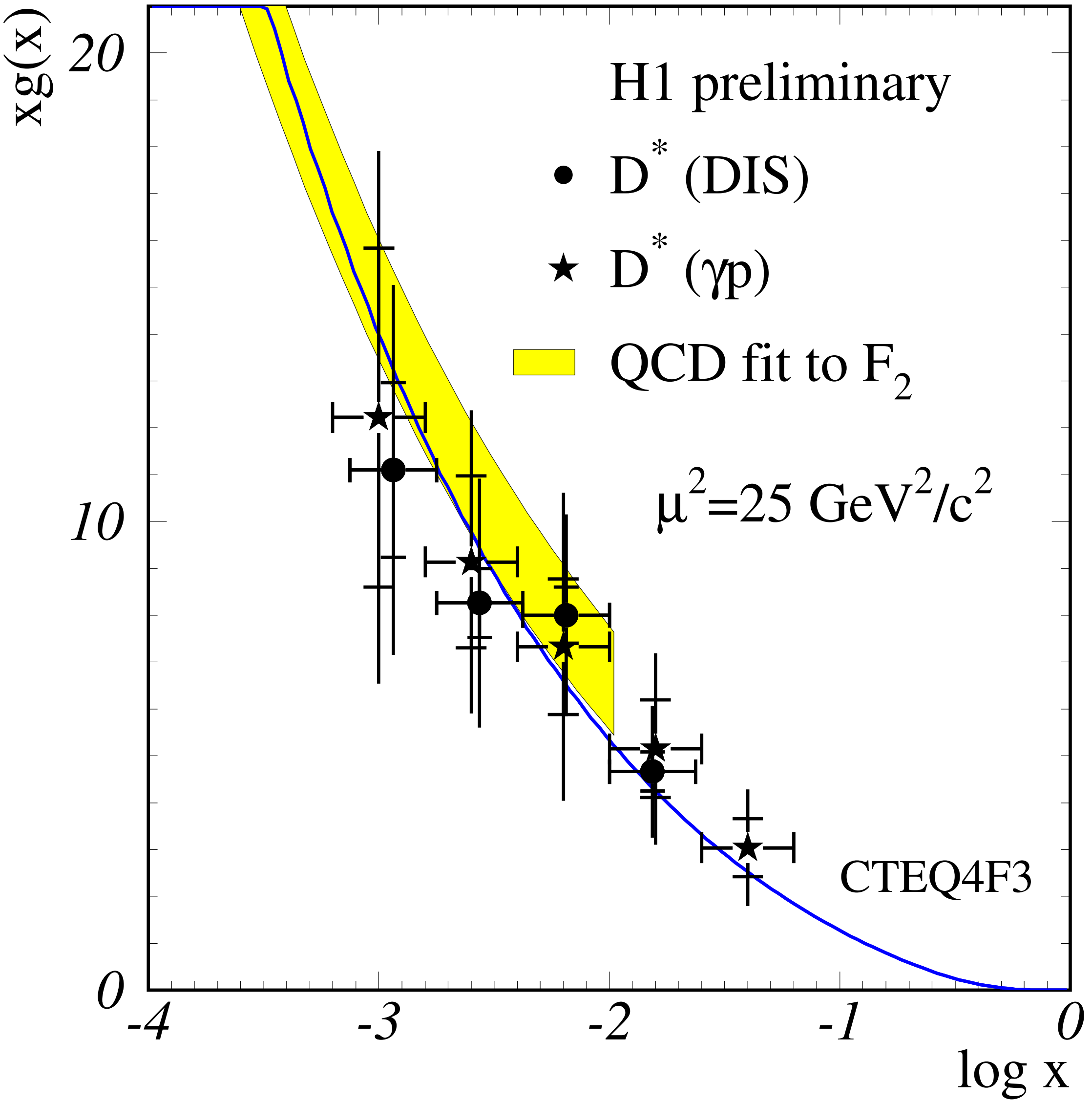

- The extraction of the gluon density from the direct measurement of the D^* production cross-section in DIS is in agreement with the gluon density obtained from the QCD fit to the inclusive cross-sections.
- Similar result from the direct measurement of the D^* production cross-section in photoproduction.

The Gluon Density from NLO QCD fit

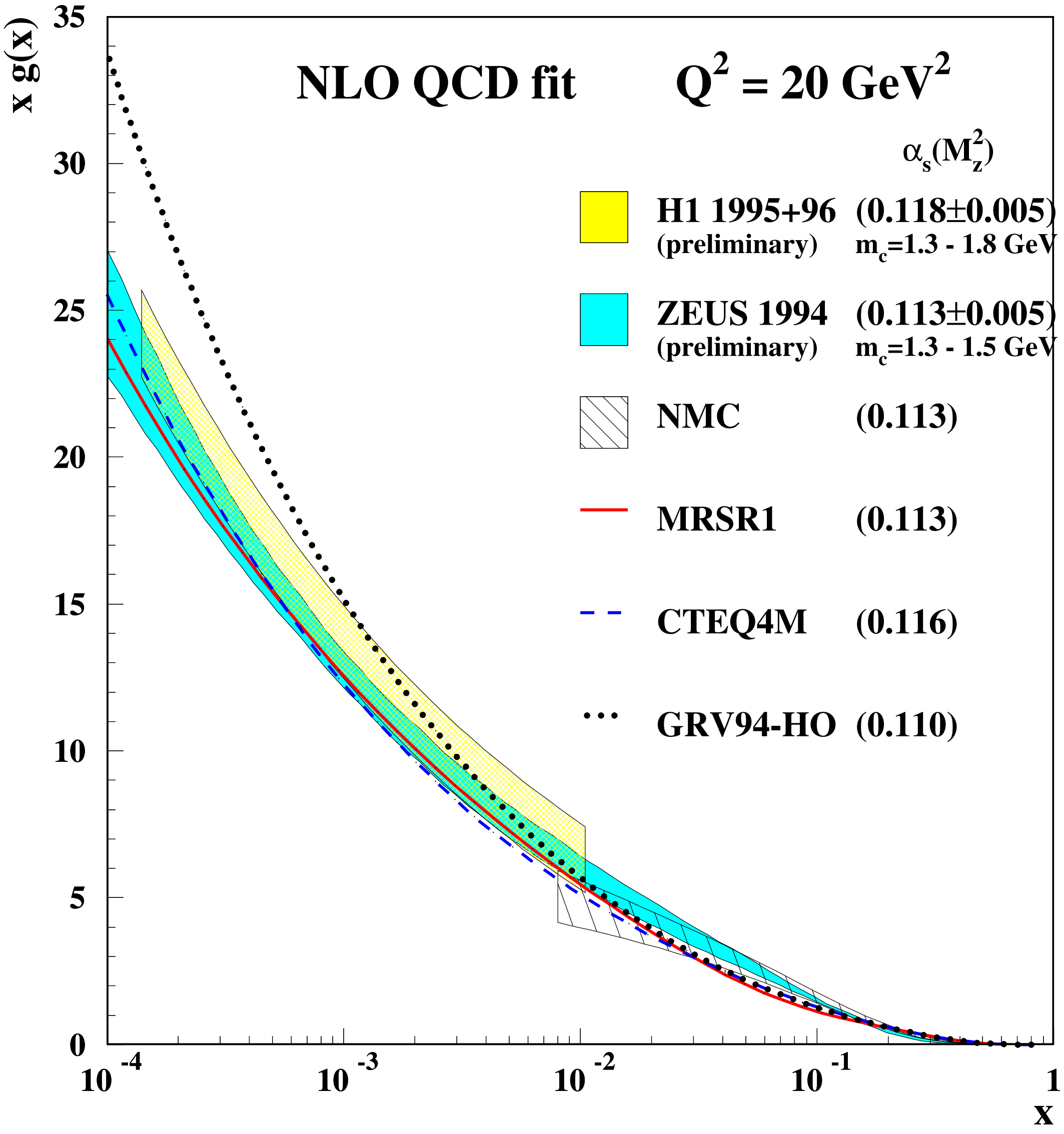

- steep rise of xg for decreasing x
- good agreement between H1 and ZEUS
- error band takes correlated systematics into account
- precision at $x \sim 5 \cdot 10^{-4}$: $\sim 15\%$
- H1 and ZEUS are consistent with MRSR1 and CTEQ4M
- GRV too steep, but uses a lower α_S value

Gluon and Sea-Quarks Densities

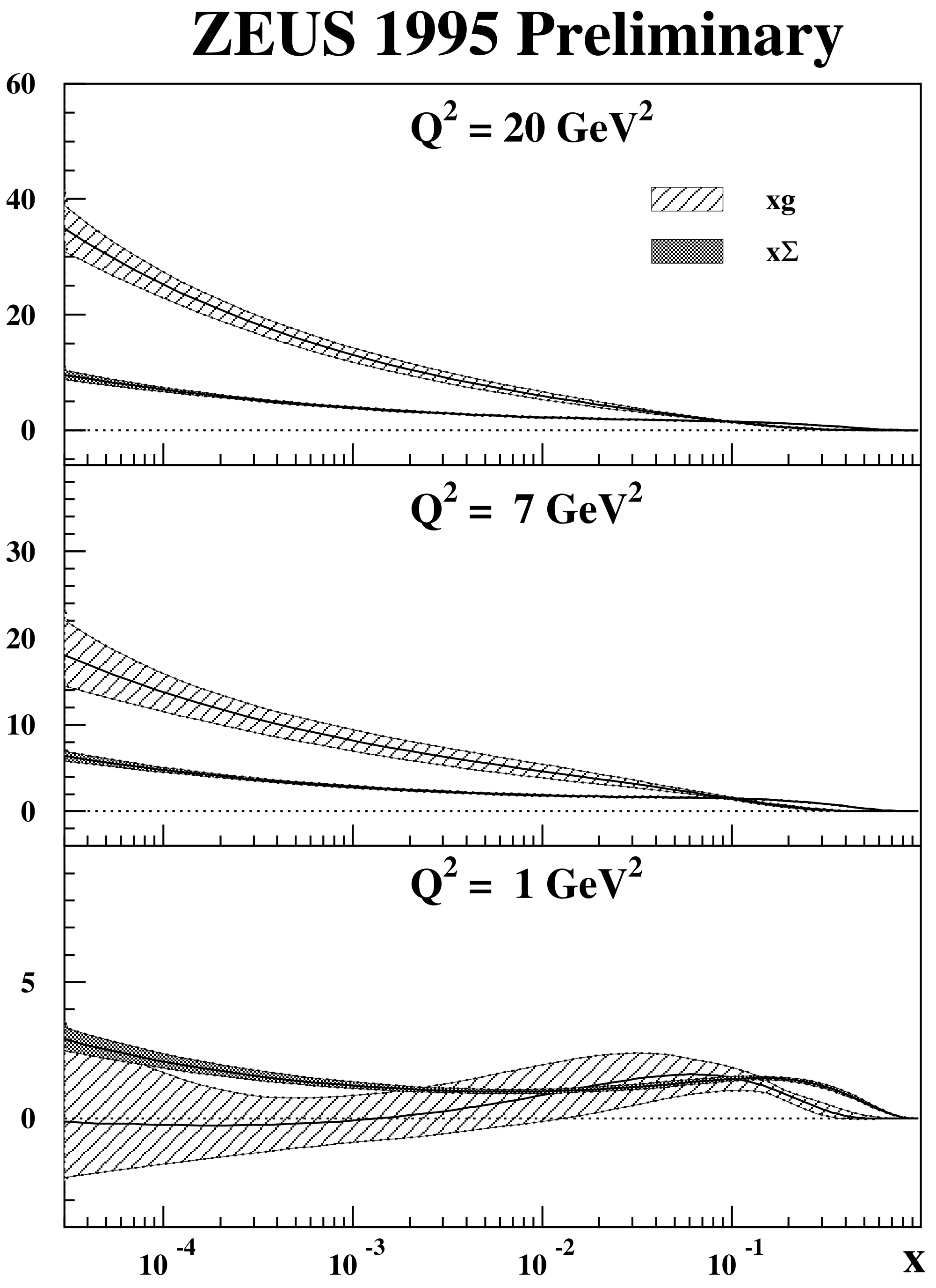

- xg is steeper at low x than the Sea-quarks density at Q^2 greater than a few GeV^2
- xg is almost flat at 1 GeV^2, while the Sea-quarks density is already increasing at low x
- Difference of dynamics at $Q^2 \lesssim 1$ GeV^2 ?

The Gluon from the Dijet Cross-Section

fit: $$\frac{d^2\sigma_{dijet}}{dQ^2 d\xi} \quad \text{with} \quad \xi = x\left(1 + \frac{M_{jj}^2}{Q^2}\right)$$

and $$\frac{d^2\sigma}{dx\,dQ^2}$$

data $200 \leq Q^2 \leq 5000$ GeV^2

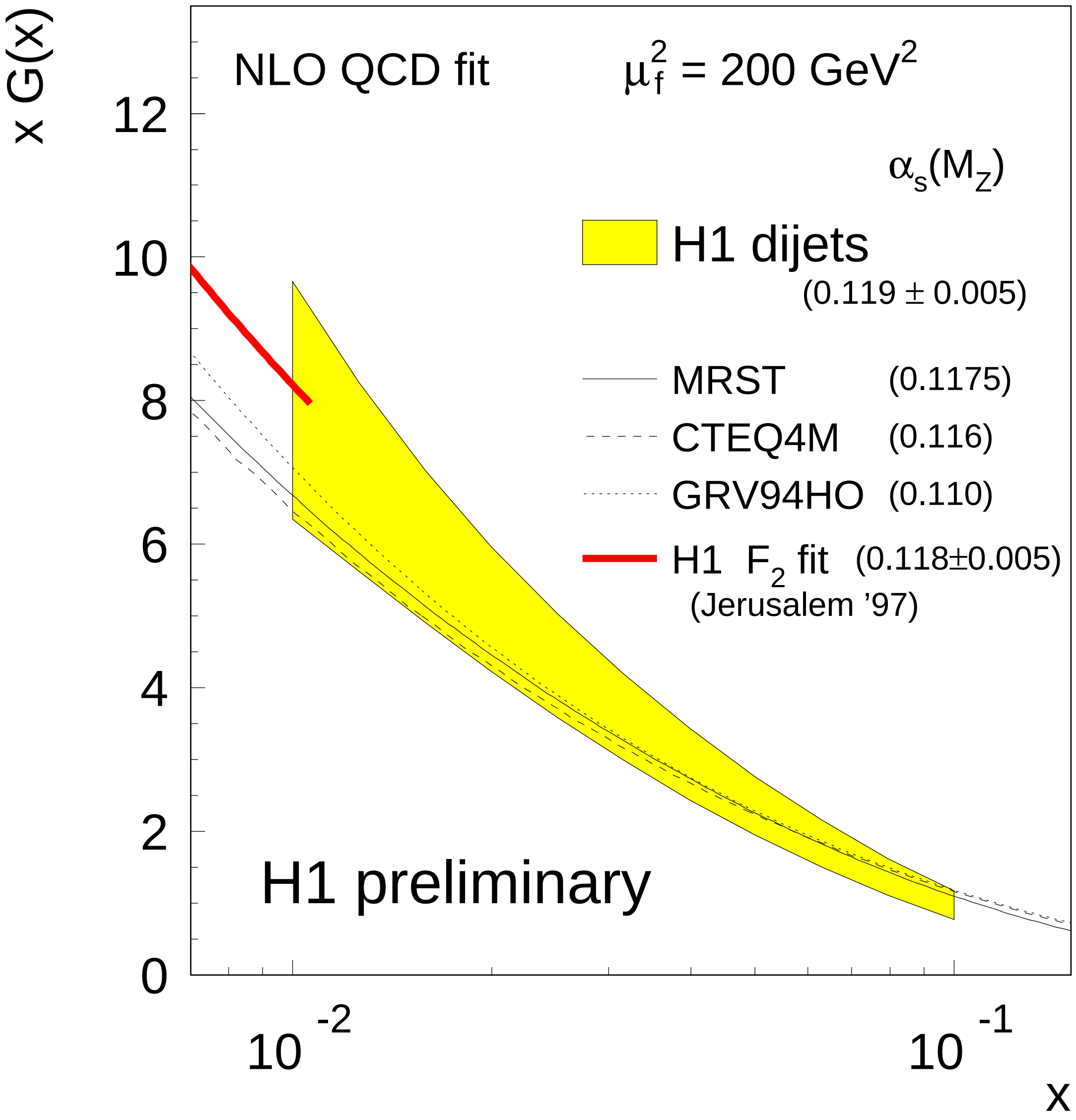

Gluon density obtained at higher x values is consistent with xg determined from inclusive measurements at low x .

Jets at HERA

- Jets
  - → Gluon density from jets
  - → Jet shapes in DIS
  - → Measurement of α_S:
    - from integrated jet rates
    - from differential jet rates
    - from event shapes

Processes in $O\,(\alpha_s)$

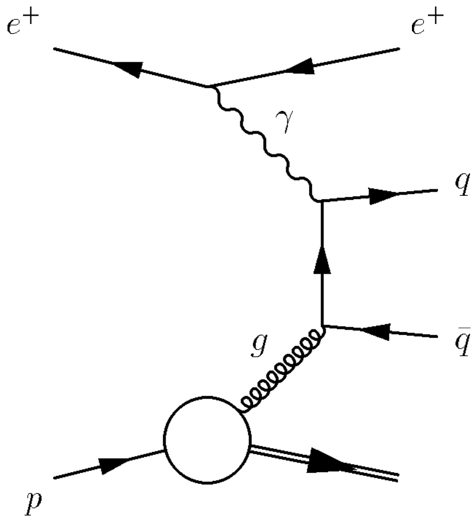

Boson–Gluon–Fusion

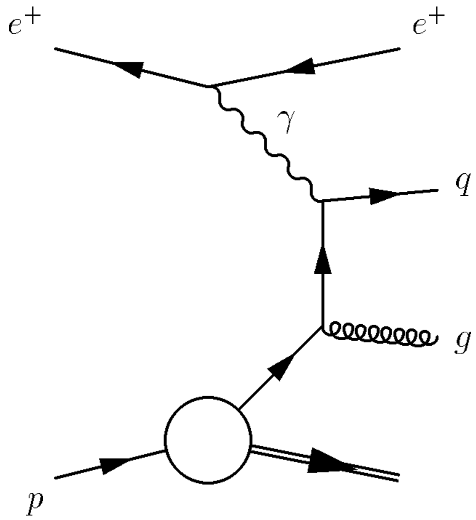

QCD–Compton

Jet shape variable

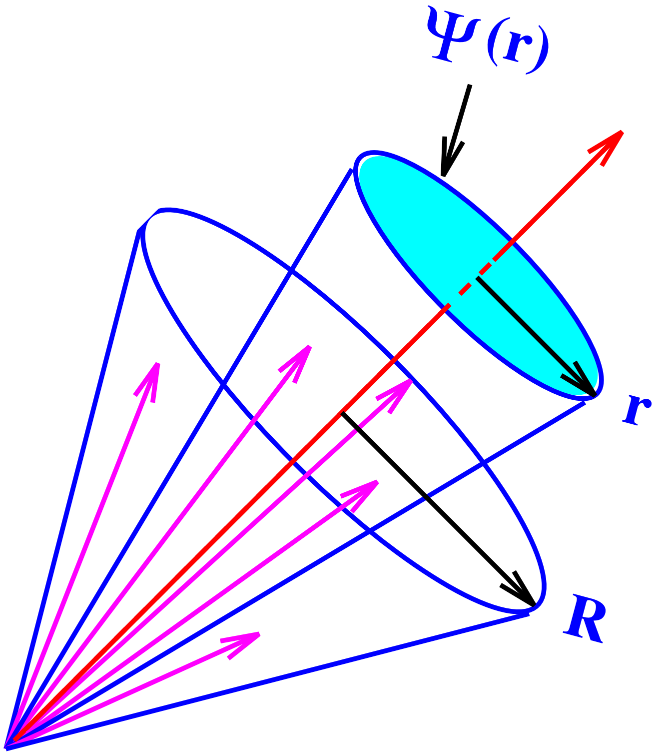

- $\Psi(r)$: average fraction of transverse jet energy contained in a cone of radius r
- by construction: $\Psi(r = R) = 1, \quad \Psi(r = 0) = 0$

Jet selection

- (CDF) cone algorithm, cone radius $R = 1$
- the jets are constructed from calorimeter energy depositions
- $-1 < \eta^{jet} < 2$

Comparison with e^+e^- and $p\bar{p}$

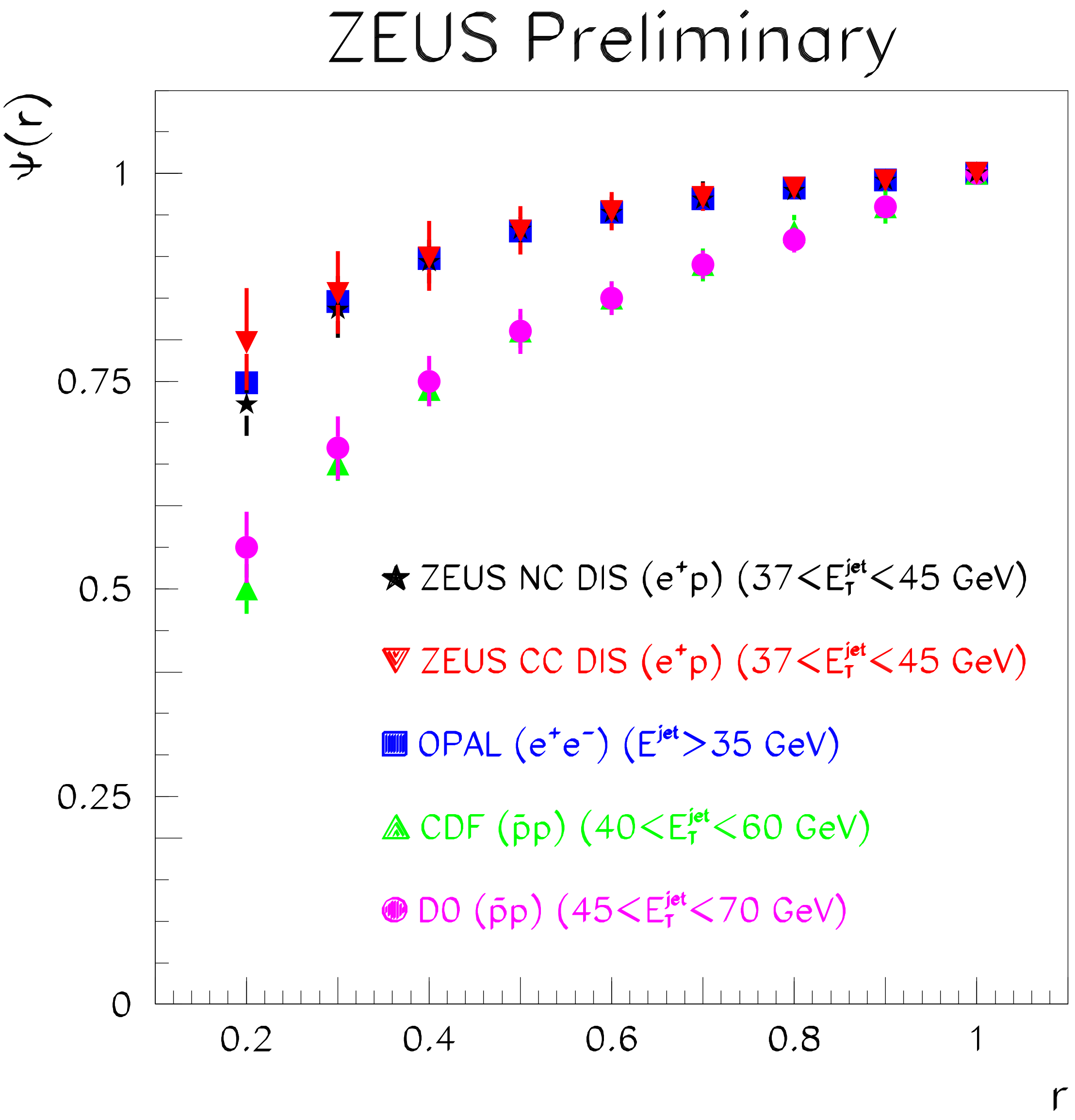

- selection of jets with comparable (transverse) energies
  ZEUS (DIS) and OPAL: mostly quark jets
  CDF and D0: mostly gluon jets
- jet profiles from ZEUS are very similar to OPAL
- jet shapes from ZEUS/OPAL are significantly narrower than those from CDF/D0

Comparison of DIS and Photoproduction

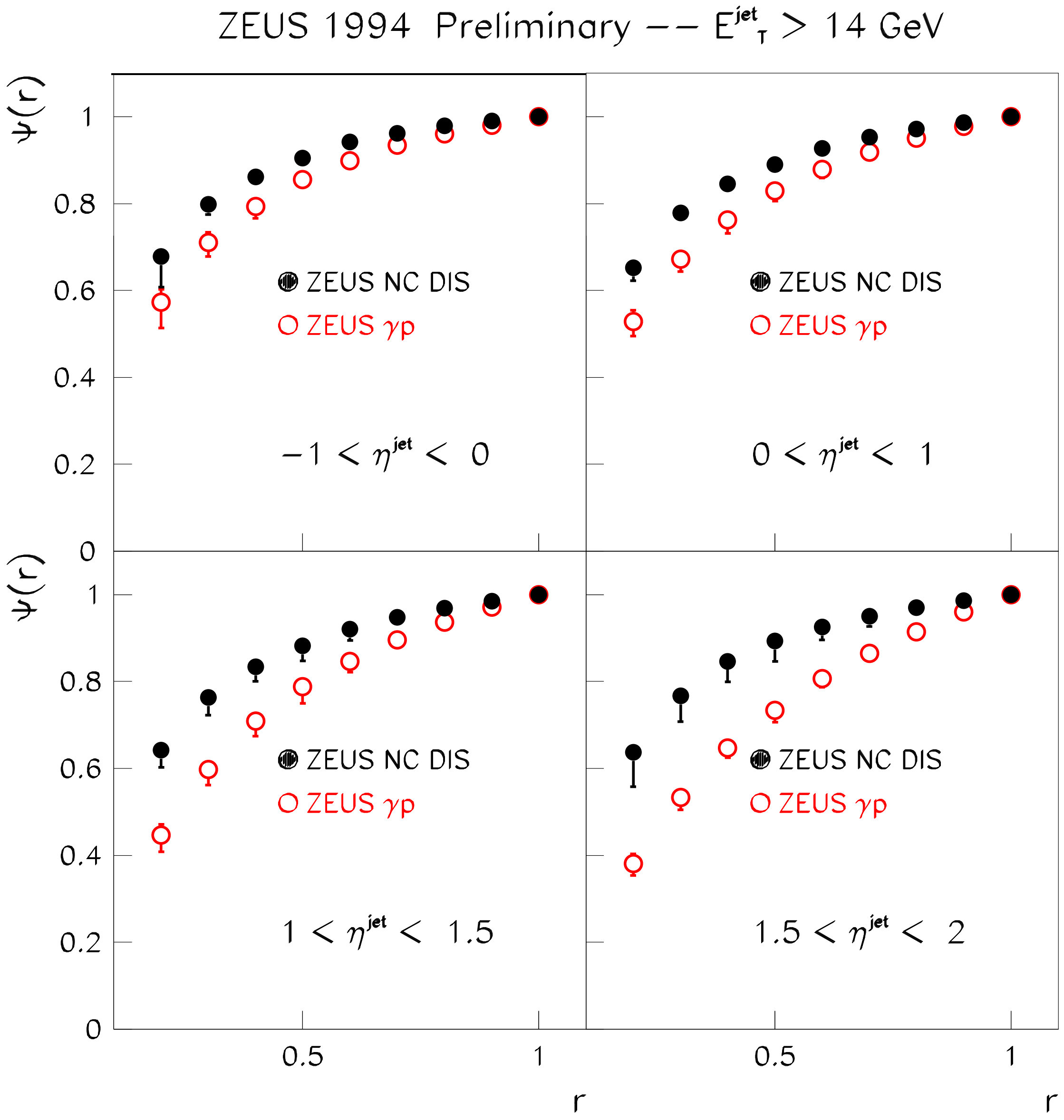

average over jets with $E_t > 14$ GeV

- clear difference between jets from DIS and photoproduction
- diffference increases with η^{jet}
- interpretation: gluon jets from resolved photoproduction dominant at large η^{jet}

(JADE) Jet Algorithm

- remove scattered electron;
  add missing momentum ‘pseudo particle’

  successive combination of pairs of particles/clusters

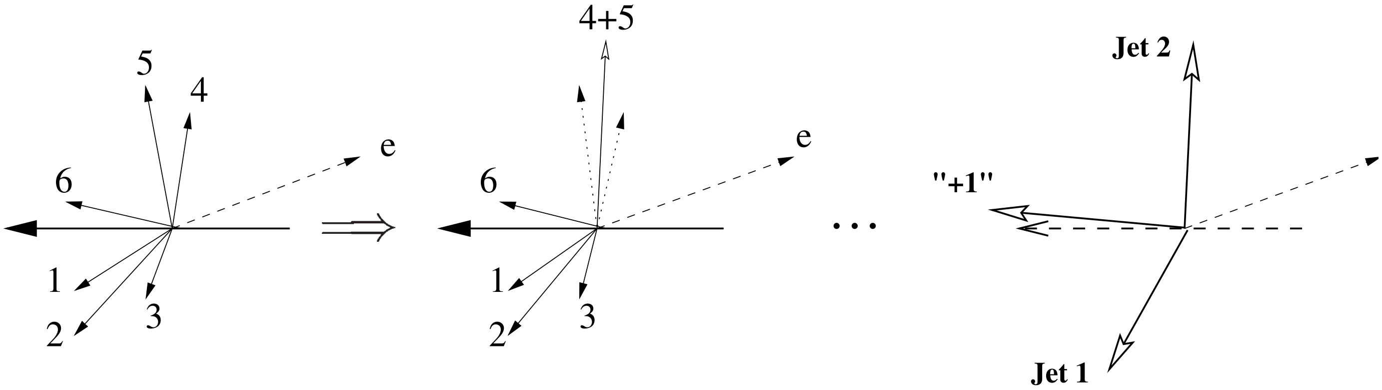

- which particles are combined ?

  ‘distance/resolution criterion’ d_{ij}^2 JADE: $d_{ij}^2 = 2E_iE_j(1 - \cos\theta_{ij})$

- in which way are the particles combined ?

  ‘recombination scheme’ JADE: $p_{comb} = p_i + p_i$

- when does the iteration stop ?

  ‘integrated’ jet rate: no pair of particles/jets is left
  with $d_{ij}^2/W^2 < y_{cut}$; $R_{2+1}(Q^2) \equiv N_{2+1}(Q^2)/N_{DIS}(Q^2)$

  ‘differential’ jet rate: (2+1) jets are left; $y_2 \equiv \min d_{ij}^2/W^2$

'Integrated' (2+1) jet rate $\boldsymbol{R_{2+1}(Q^2)}$

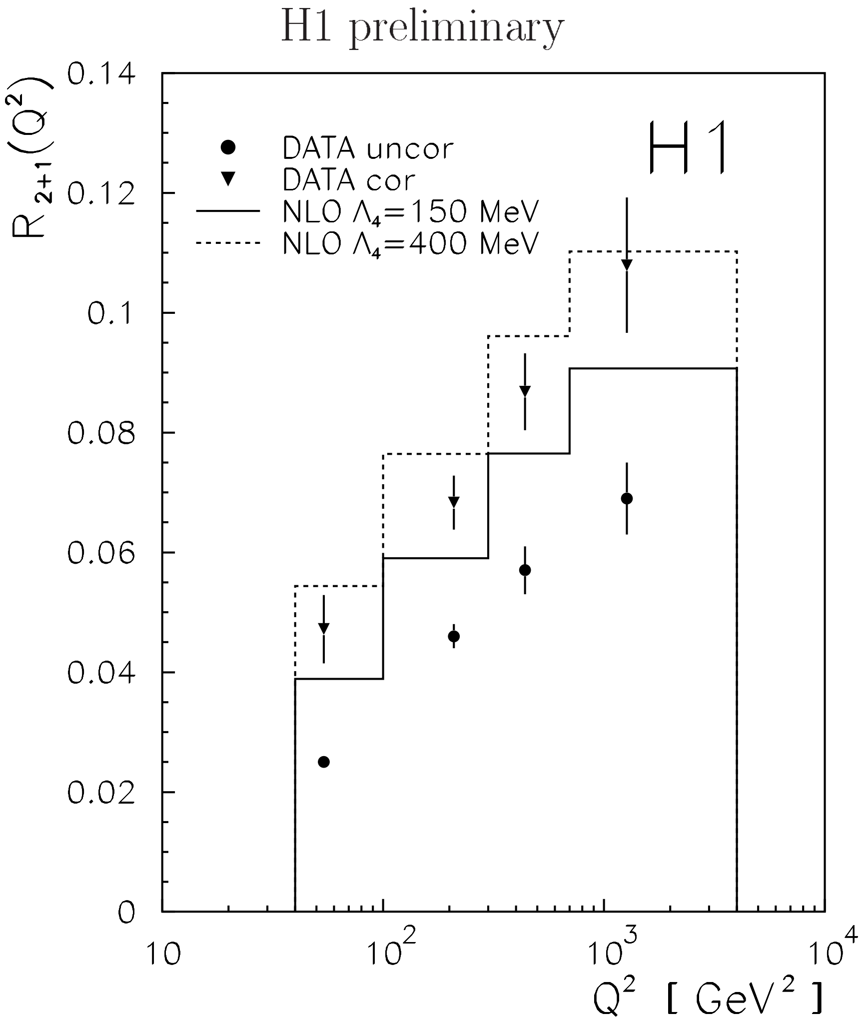

- the 3-jet rate $R_3(s)$ in e^+e^- annihilation is **the method** to measure the running of α_S!

- **aim at HERA:** demonstration of the running of α_S with one method in one experiment to minimize the systematic uncertainties by measuring $R_{2+1}(Q^2)$

- Correction factors for detector and hadronization effects are (still) large: $\sim 1.5 - 1.9$ in particular at low Q^2
- $R_{2+1}(Q^2)$ rises with increasing Q^2:

  $$R_{2+1}(Q^2) = A(Q^2, y_{cut}\alpha_s(Q^2) + B(Q^2, y_{cut})\alpha_S^2(Q^2)))$$

  in $e^+e^- \to q\bar{q}g$: $R_3(y_{cut}) = A(y_{cut})\alpha_S(s) + B(y_{cut})\alpha_S^2(s)$
- Choice of renormalisation scale μ_R^2 in bin i is $\langle Q^2\rangle_i$

'Running' of $\boldsymbol{\alpha_S(Q^2)}$ from $\boldsymbol{R_{2+1}(Q^2)}$

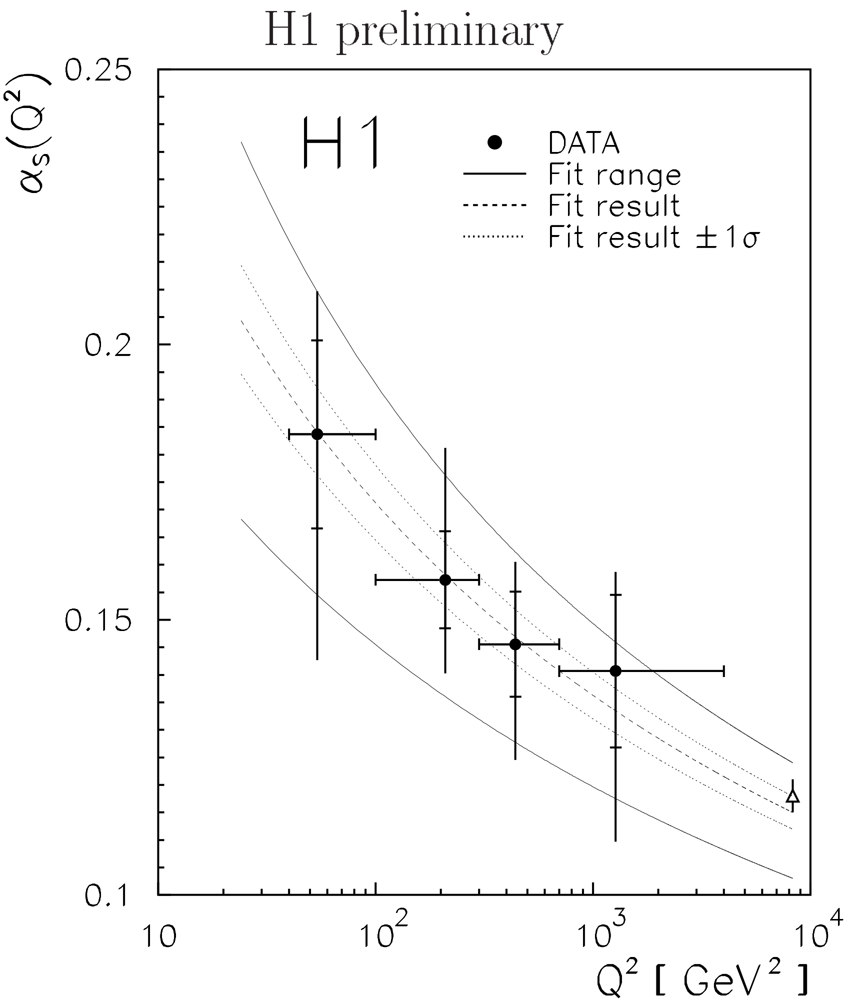

- result of α_s fit to R_{2+1}:
  4 values of $\alpha_s(< Q^2 >)$ corresponding to 4 bins of Q^2
- systematic uncertainties are largest at low Q^2
- (still) large statistical error at very high Q^2
  ($\Delta\alpha_s \sim 10\%$ for $700 < Q^2 < 4\,000$ GeV^2)
- unambiguous demonstration of 'running' of α_s is not (yet) possible
- averaging over full range of Q^2, we get:
  $\alpha_s(M_Z) = 0.115 \pm 0.003\ (stat.)\ ^{+0.008}_{-0.011}\ (syst.)$

'Differential' (2+1) Jet Rate

- differential 3–jet rates have been studied in much detail in e^+e^-–annihilation

- this is the first study of the corresponding variable in *ep*

  e^+e^-: *fixed* $s \Leftrightarrow$ ep: *range* of Q^2

- y_2 is complementary to $R_{2+1}\,(Q^2)$ at *fixed* jet resolution parameter y_{cut}

  within a given Q^2 range: $-\frac{dR_{2+1}}{dy_{cut}} = -\frac{1}{N_{tot}} \cdot \frac{dN_{2+1}}{dy_{cut}} \approx \frac{1}{N_{tot}} \cdot \frac{dN}{dy_2}$

- only the combined study of y_2 and $R_{2+1}\,(Q^2)$ gives the full picture of (2+1) jet rates at HERA

- analysis is restricted to $Q^2 > 200$ GeV^2

  $\Rightarrow$ reduced systematic uncertainties due to:
  suppression of initial–state QCD radiation;
  improved containment of jets in detector;
  better knowledge of parton densities at high x;
  …

α_s from Differential Jet Rate

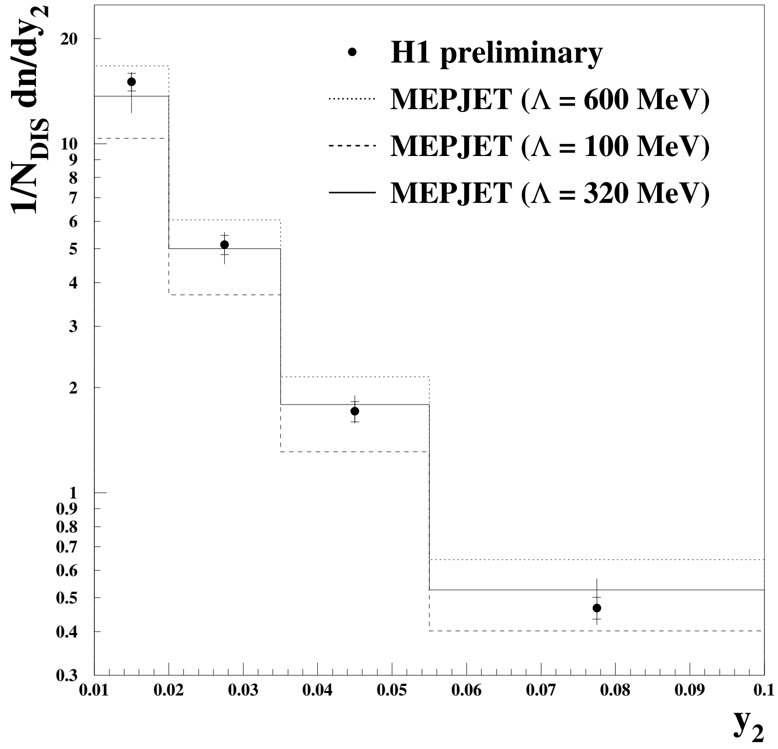

- $\Lambda^{(4)}_{\overline{MS}}$ is fitted to the corrected data considering statistical correlation between bins
- the fit result is:
  $\alpha_S(M_Z) =$
  $0.118 \pm 0.002(stat)^{+0.007}_{-0.008}(syst)^{+0.007}_{-0.006}(theo)$
  corresponding to $\Lambda^{(4)}_{\overline{MS}} = 320 \pm 33$ MeV
- QCD in NLO and corrected data agree for α_S^{fit}
- largest uncertainties due to:
  - the model dependence (LEPTO, ARIADNE, HERWIG...)
  - the parton densities
  - the renormalisation scale ambiguity ($\mu_R^2 = Q^2 \rightarrow 1/4 \quad \text{and} \quad 4Q^2$)

DIS Event Shapes in the Breit Frame

- Phase Space in the Current Hemisphere of the Breit Frame for $e\,p \to e\,X$ Events:

$$Q/2$$

- Phase Space in one Hemisphere of $e^+e^- \to q\,\bar{q}$ Events:

$$\sqrt{s}/2$$

⇒ **Is there a relation between $e\,p$ Scattering and e^+e^- Annihilation concerning Event Shapes at a Scale:**

$$Q_{DIS} = \sqrt{s_{ee}}\ ?$$

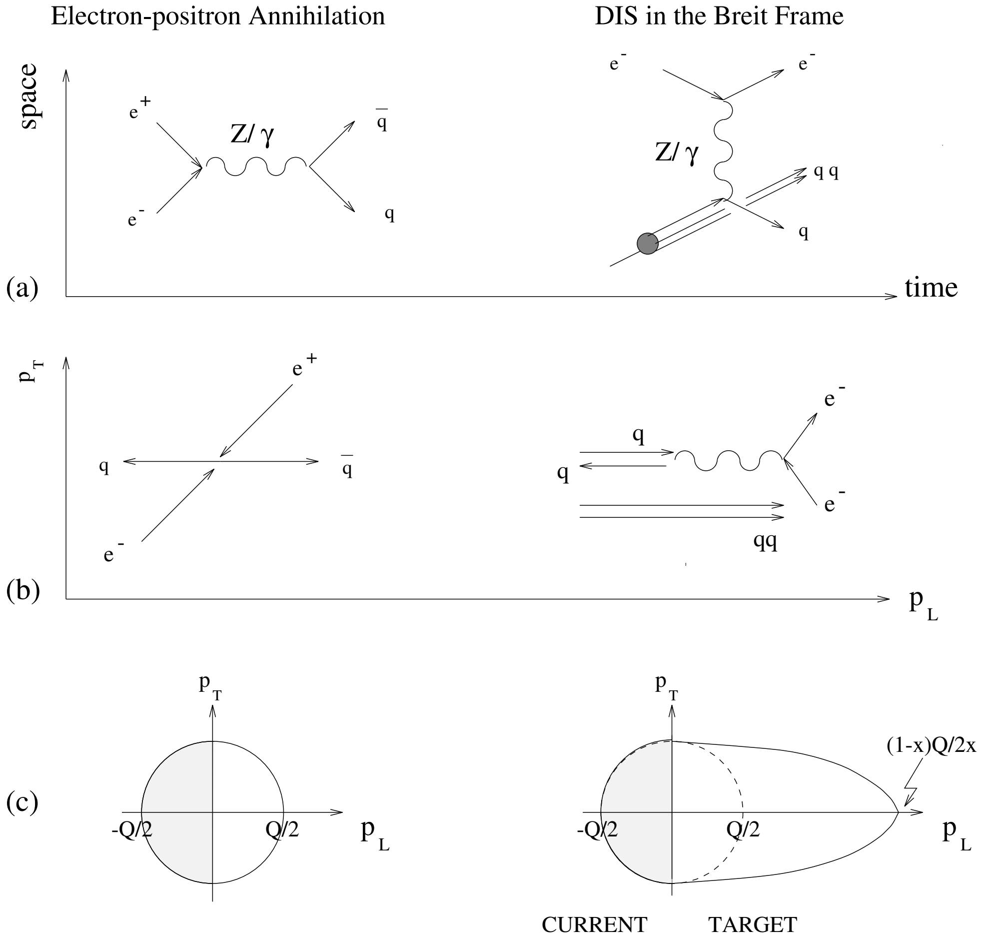

Power Corrections and $\alpha_s(M_Z)$

- **Q or energy dependence of event shape variables**

  (i) change of strong coupling constant $\alpha_s(Q) \propto 1/\ln(Q/\Lambda)$

  (ii) power or so-called ‘hadronisation’ corrections $\propto 1/Q$

- **Mean value of any infrared safe event shape variable $\langle F \rangle$**

  (e.g. $F = 1 - T_c,\ (1 - T_z)/2,\ B_c,\ \rho_c$)

  can be written in DIS $e\,p$ and in e^+e^- annihilation as:

$$\langle F \rangle \quad = \quad \langle F \rangle^{\rm pert} + \langle F \rangle^{\rm pow}$$

  - Perturbative part:

$$\langle F \rangle^{\rm pert} \quad = \quad c_1\,\alpha_s(Q) + c_2\,\alpha_s^2(\mu_R)$$

  → **coefficients $c_1,\ c_2$ from $\mathcal{O}(\alpha_s^2)$ DISENT calculations**

  - Power corrections:

$$\langle F \rangle^{\rm pow} \quad = \quad a_F\,\frac{16}{3\,\pi}\,\frac{\mu_I}{Q}\,\ln^p\frac{Q}{\mu_I}\left[\bar{\alpha}_0(\mu_I) - \alpha_s(Q) - \frac{\beta_0}{2\,\pi}\left(\ln\frac{Q}{\mu_I} + \frac{K}{\beta_0} + 1\right)\alpha_s^2(Q)\right]$$

Dokshitzer,Webber: $1/Q$ corrections not necessarily related to hadronisation. Power corrections may be due to a “universal” soft gluon phenomenon associated with the behaviour of the running coupling at small momentum scales. “Universal” means that they could be expressible in terms of a few non-perturbative parameters with calculable process dependent coefficients a_F and p.

→ **contain a non-perturbative parameter** $\bar{\alpha}_0(\mu_I)$

to be evaluated at some ‘infrared matching’ scale: $\Lambda \ll \mu_I \ll Q$

- **QCD Analysis of $\langle F \rangle$ → $\bar{\alpha}_0$ and $\alpha_s(M_Z)$**
  - **Power corrections $\propto 1/Q$ for all $\langle F \rangle$**
  - **Universal power correction parameters $\bar{\alpha}_0$ for all $\langle F \rangle$**

Event Shape Variables in the Breit Current Hemisphere

- **Thrust T_c**

$$T_c \quad = \quad \max \frac{\sum_h |\, \mathbf{p}_h \cdot \mathbf{n}_T \,|}{\sum_h |\, \mathbf{p}_h \,|} \qquad\qquad \mathbf{n}_T \;\equiv\; \text{thrust axis}$$

- **Thrust T_z** closer to $e^+ e^-$ annihilation

$$T_z \quad = \quad \frac{\sum_h |\, \mathbf{p}_h \cdot \mathbf{n} \,|}{\sum_h |\, \mathbf{p}_h \,|} \quad = \quad \frac{\sum_h |\, \mathbf{p}_{z\,h} \,|}{\sum_h |\, \mathbf{p}_h \,|} \qquad\qquad \mathbf{n} \;\equiv\; \text{hemisphere axis}$$

- **Jet Broadening B_c**

$$B_c \quad = \quad \frac{\sum_h |\, \mathbf{p}_h \times \mathbf{n} \,|}{2\, \sum_h |\, \mathbf{p}_h \,|} \quad = \quad \frac{\sum_h |\, \mathbf{p}_{\perp\,h} \,|}{2\, \sum_h |\, \mathbf{p}_h \,|} \qquad\qquad \mathbf{n} \;\equiv\; \text{hemisphere axis}$$

- **Jet Mass ρ_c**

$$\rho_c \quad = \quad \frac{M^2}{Q^2} \quad = \quad \frac{(\, \sum_h \, p_h \,)^2}{Q^2}$$

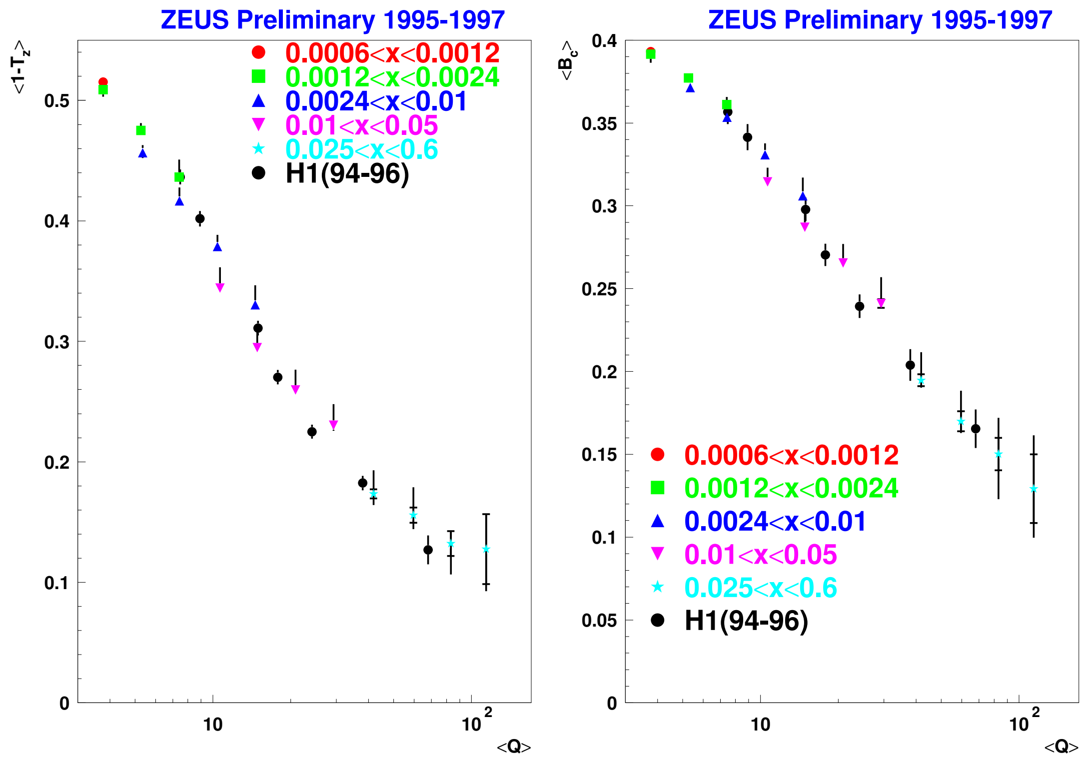

Results of QCD fits and Conclusions

Observable	$\bar{\alpha}_0(\mu_I = 2\ \mathrm{GeV})$	$\alpha_s(M_Z)$	χ^2/ndf
H1 $e\,p$ data			
$\langle 1-T_c \rangle$	$0.481 \pm 0.005\ ^{+0.109}_{-0.036}$	$0.123 \pm 0.002\ ^{+0.007}_{-0.005}$	5.1/5
$\langle 1-T_z \rangle\,/\,2$	$0.492 \pm 0.010\ ^{+0.109}_{-0.051}$	$0.115 \pm 0.002\ ^{+0.007}_{-0.005}$	8.1/5
$\langle B_c \rangle$	$0.375 \pm 0.008\ ^{+0.036}_{-0.022}$	$0.116 \pm 0.002\ ^{+0.007}_{-0.004}$	5.3/5
$\langle \rho_c \rangle$	$0.454 \pm 0.009\ ^{+0.025}_{-0.020}$	$0.130 \pm 0.003\ ^{+0.007}_{-0.005}$	2.8/5
common fit			
$T_c + T_z + \rho_c$	$\mathbf{0.491 \pm 0.003\ ^{+0.079}_{-0.042}}$	$\mathbf{0.118 \pm 0.001\ ^{+0.007}_{-0.006}}$	39/19
e^+e^- data			
$\langle 1-T_{ee} \rangle$	$0.519 \pm 0.009\ ^{+0.093}_{-0.039}$	$0.123 \pm 0.001\ ^{+0.007}_{-0.004}$	10.9/14
$\langle M_H^2/s \rangle$	$0.580 \pm 0.015\ ^{+0.130}_{-0.053}$	$0.119 \pm 0.001\ ^{+0.004}_{-0.003}$	10.9/14

- First Analysis at HERA of the DIS Event Shape Parameters $1-T_C,\ 1-T_Z,\ B_C,\ \rho_C$ in the Breit Current Hemisphere with the coverage of a large range in $Q = 7 \div 100$ GeV in a Single Experiment
- The Event Shapes become more collimated with rising Q as expected. and give consistent results. They are compatible with a Universal Power Correction Parameter $\bar{\alpha}_0 \approx 0.5$ within $\pm 20\,\%$.
- The Strong Coupling Constant $\alpha_s(M_Z)$ and $\bar{\alpha}_0$ are simultaneously determined independently of Fragmentation Models using $\mathcal{O}(\alpha_s^2)$ Calculations of DISENT and MEPJET.
- The comparison with e^+e^- Experiments shows that the Q Dependence of Thrust and Jet Masses is in gross agreement despite differences in the underlying Physics and the analysis methods. The same Power Correction Parameters $\bar{\alpha}_0$ are found within $\pm 20\,\%$ of $e\,p$ results.

DIS Events at High Q^2

High Q^2 Neutral Current (NC)

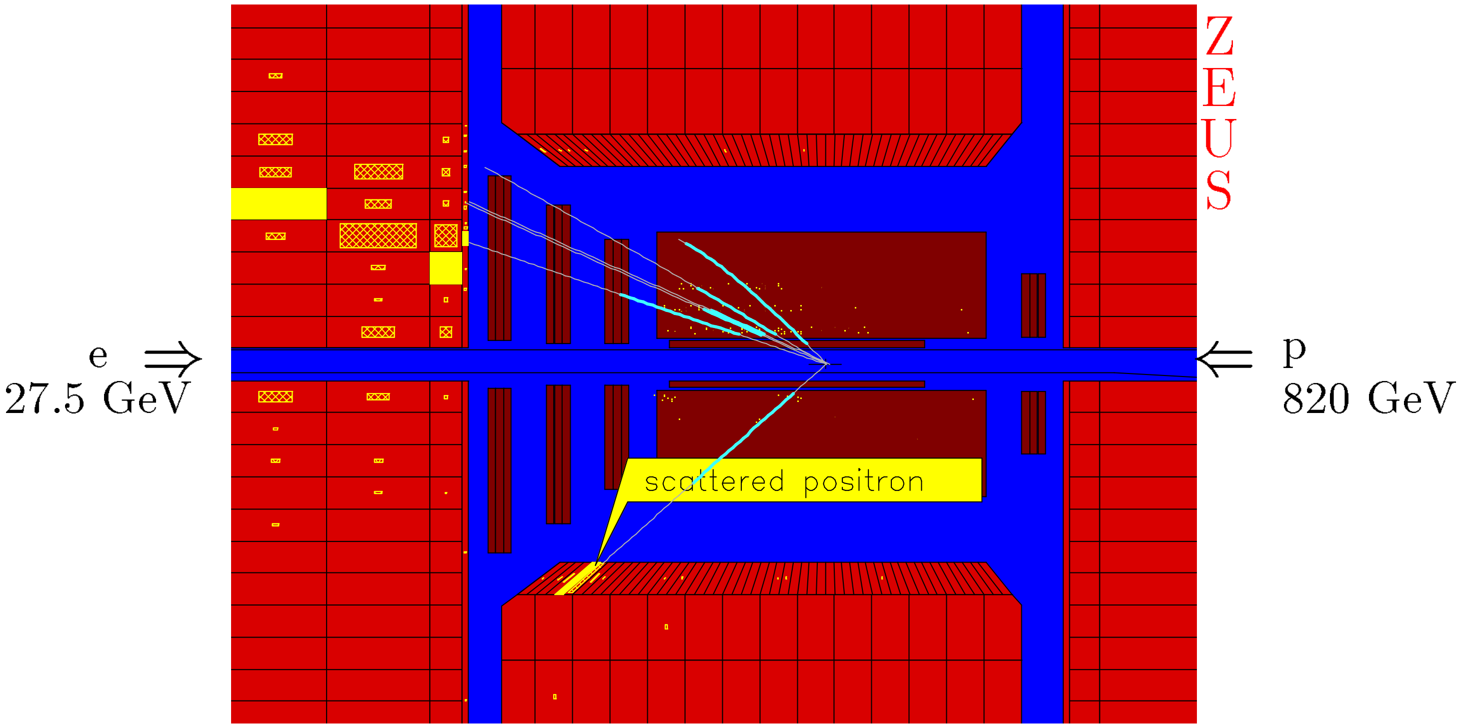

High Q^2 Charged Current (CC)

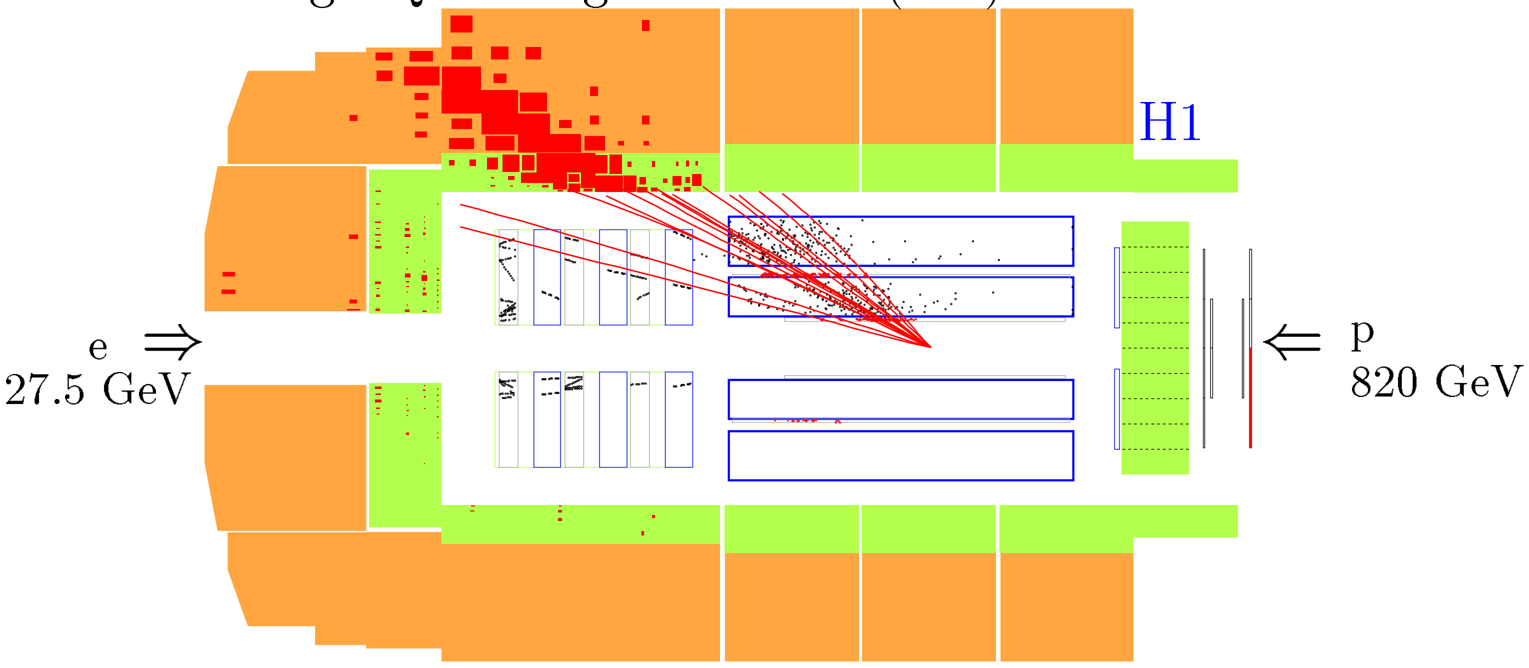

$\mathrm{d}\sigma/\mathrm{d}x$ at $Q^2 > 1000, 10000\ \mathrm{GeV}^2$

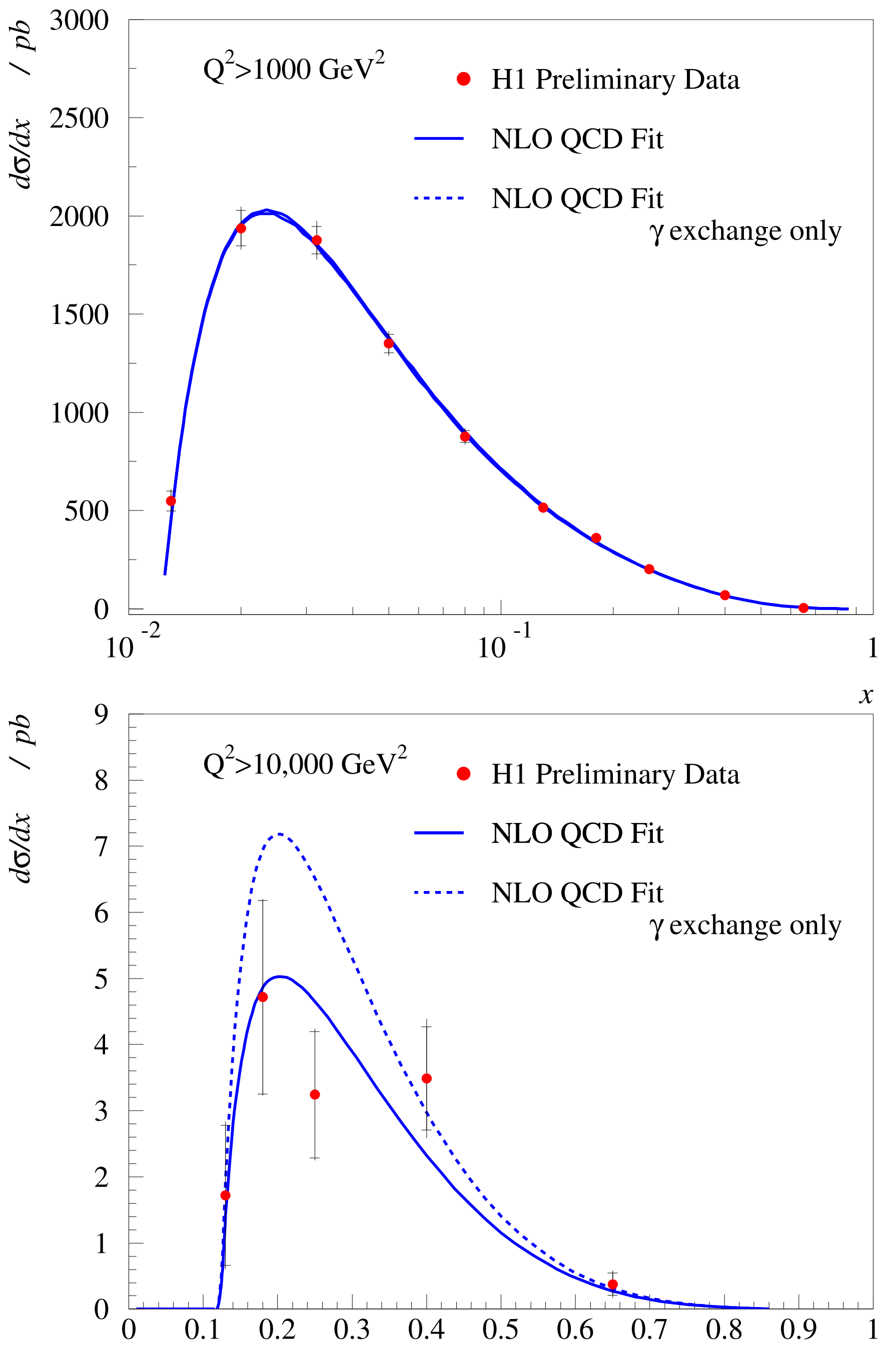

- For $Q^2 \geq 1000\ \mathrm{GeV}^2$, the cross-section is still dominated by low x parton scattering.
- For $Q^2 \geq 10000\ \mathrm{GeV}^2$ the valence quarks contribute.
- The data are in good agreement with the electroweak Standard Model. Z exchange needed!

Neutral Current Cross-Sections

Kinematic Domain: 200 GeV^2 $\leq$ Q^2 $\leq$ 30000 GeV^2
$0.005 \leq x \leq 0.65$

$$\frac{d^2\sigma^{e^+p}}{dx\,dQ^2} = \frac{2\pi\alpha^2}{xQ^4}\left[Y_+F_2(x,Q^2) - y^2F_L(x,Q^2) - Y_-xF_3(x,Q^2)\right]$$

$$Y_\pm(y) = 1 \pm (1-y)^2$$

F_2,F_3: generalized structure functions
F_L: longitudinal structure function

$$F_2 = F_2^{em} + \frac{Q^2}{(Q^2+M_Z^2)}F_2^{int} + \frac{Q^4}{(Q^2+M_Z^2)^2}F_2^{wk} = F_2^{em}(1+\delta_Z)$$

F_2^{em}: photon exchange
F_2^{wk}: Z° exchange
F_2^{int}: γZ° interference

In the following we will use the Reduced Cross-Section:

$$\tilde{\sigma}(e^+p) \equiv \frac{xQ^4}{2\pi\alpha^2}\frac{1}{Y_+}\frac{\mathrm{d}^2\sigma}{\mathrm{d}x\mathrm{d}Q^2}$$

$$\approx F_2^{em}(1+\delta_Z-\delta_3-\delta_L)$$

$\delta_Z - \delta_3$: $<$ 1% at Q^2 $<$ 1500 GeV^2
$\approx$ 10% at Q^2 = 5000 GeV^2 and x=0.08

δ_L: negligible at $y < 0.5$
$\approx$ 5% at $y = 0.9$

Contributions to the NC Cross-Section

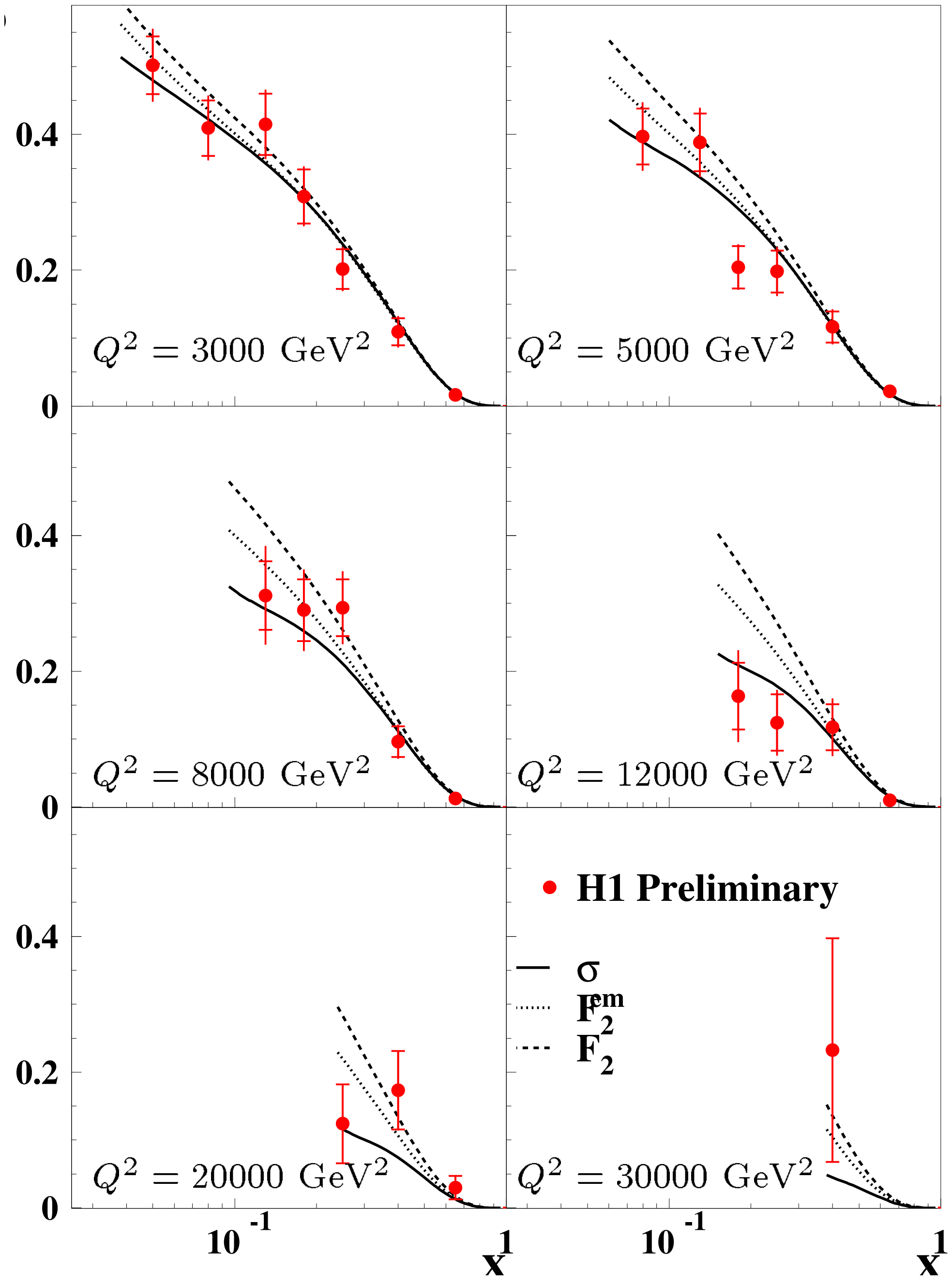

$\Rightarrow$ **at $Q^2 \geq 15000$ GeV^2**
no structure function
has a dominant contribution!

Reduced Neutral Current Cross-Section

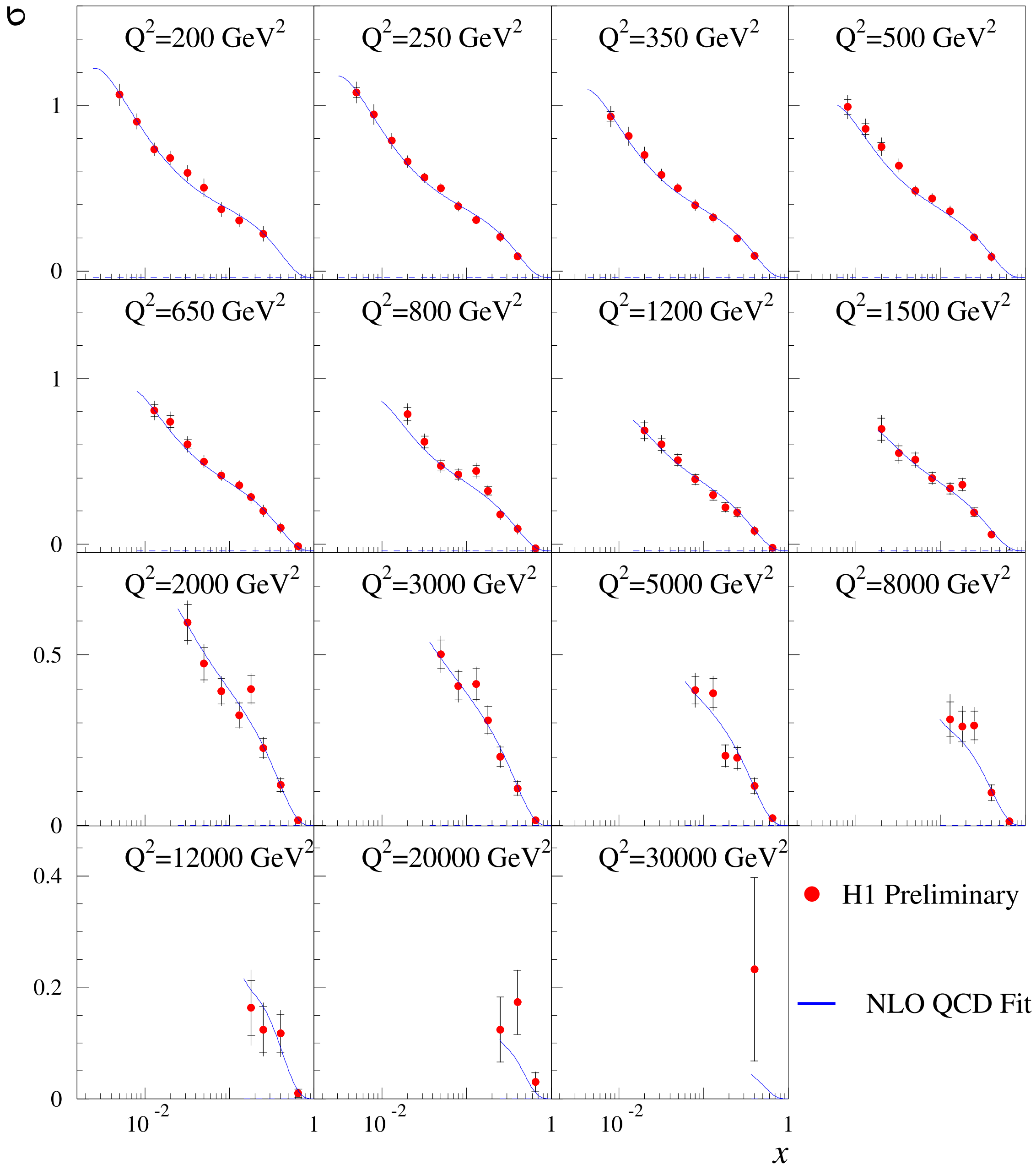

- Measurement from $Q^2 = 200$ to 30000 GeV^2, up to $x = 0.65$ for $Q^2 \geq 650$ GeV^2.
- NLO QCD fit gives good description of the data in the whole Q^2 and x range
- Precision limited by statistics at $Q^2 > 1000$ GeV^2
- total error (syst $\oplus$ stat) $< 10\%$ except at high Q^2

Reduced Cross-Section at High $\boldsymbol{x}$

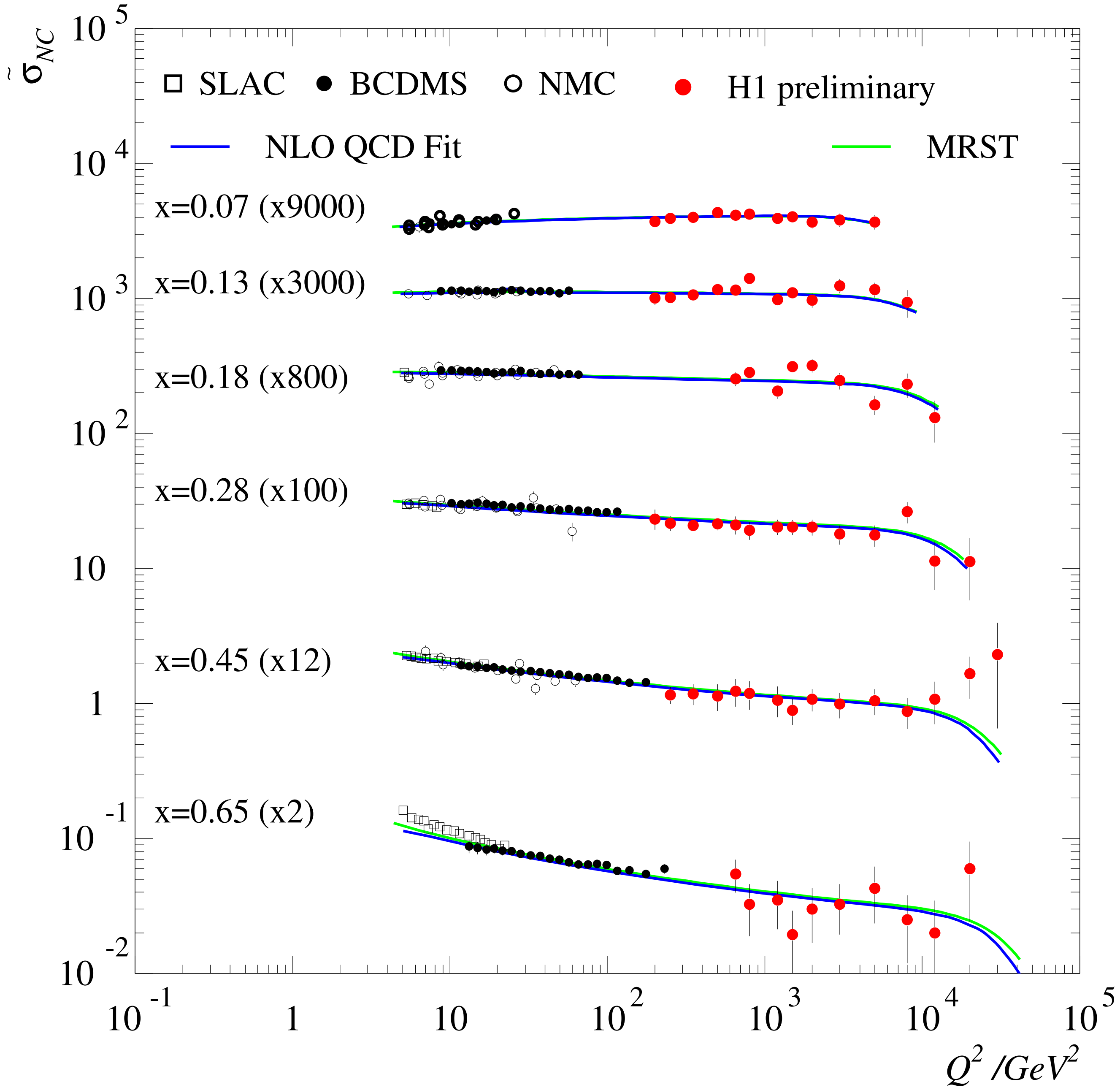

- Difference visible in the QCD fit when the high Q^2 data is or is not included.
- High Q^2 HERA data now also have an influence at **high** x **(**$\approx 5\%$ **at highest** Q^2).
- α_S measurement from $dF_2/d\ln Q^2$ at high x in future.

Charged Current Cross-Sections

Cross Section for $e^+p \longrightarrow \bar{\nu}X$:

$$\frac{d^2\sigma}{dxdQ^2} = \frac{G_F^2}{2\pi}\frac{1}{(1+Q^2/M_W^2)^2}\left(\bar{u}+\bar{c}+(1-y)^2(d+s)\right)$$

- Propagator dependence ⇒ W mass determination

  H1 (94-97): $81.2{\scriptstyle \pm 3.3 \pm 4.3}$ GeV

  ZEUS (94-97): $78.6^{+2.5+3.3}_{-2.4-3.0}$ GeV

- parton densities ⇒ sensitivity to d-quark density
- helicity dependence ⇒ V-A coupling
- QED radiative Corrections ($<10\%$) applied

Reduced Charged Current Cross-Section:

$$\begin{aligned} \sigma_{CC} &\equiv x \cdot \frac{2\pi}{G_F^2}(1+Q^2/M_W^2)^2\frac{d^2\sigma}{dxdQ^2} \\ &= x \cdot (\bar{u}+\bar{c}+(1-y)^2(d+s)) \; in \; QPM \end{aligned}$$

- definition in analogy to the Reduced Neutral Current Cross-Section
- different relation to the parton densities: supression of the valence quark contribution at high y due to the helicity factor

The propagator Mass M_W

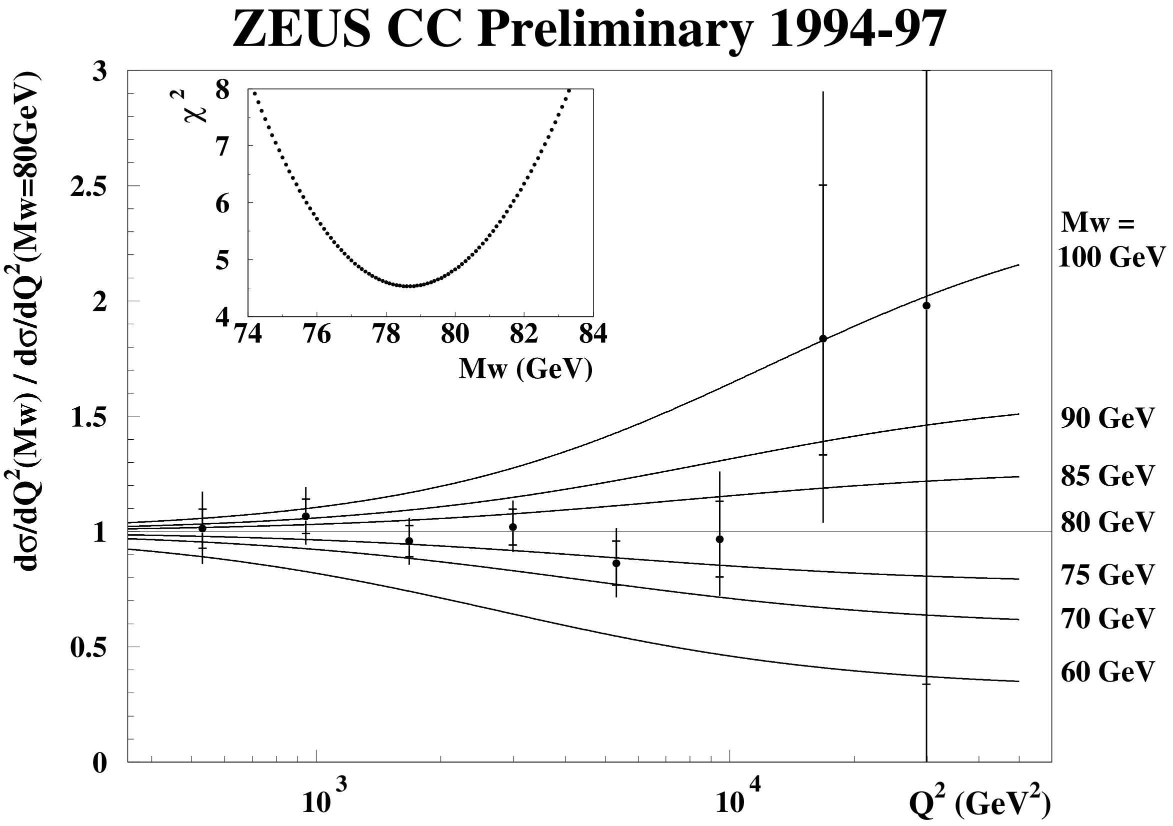

- The Q^2 dependence of the CC cross-section is determined by the propagator mass (and the parton densities).

ep : space-like measurement of M_W

$\Leftrightarrow$ $e^+e^-, p\bar{p}$: time-like measurement of M_W

$$\frac{d^2\sigma_{CC}}{dx dQ^2} = \frac{G_F^2}{2\pi x} \cdot \left(\frac{M_W^2}{M_W^2 + Q^2} \right)^2 \cdot \phi_{CC}(x, Q^2)$$

- input parameters: $\alpha, M_W, M_Z, M_{top}, M_H$
- parton densities: MRST (H1)/ CTEQ4D (ZEUS)

H1 (94-97): $81.2 \pm 3.3 \pm 4.3$ GeV

ZEUS (94-97): $78.6^{+2.5+3.3}_{-2.4-3.0}$ GeV

- in agreement with $M_W = 80.41 \pm 0.10$ GeV from pdg

CC reduced Cross-Section

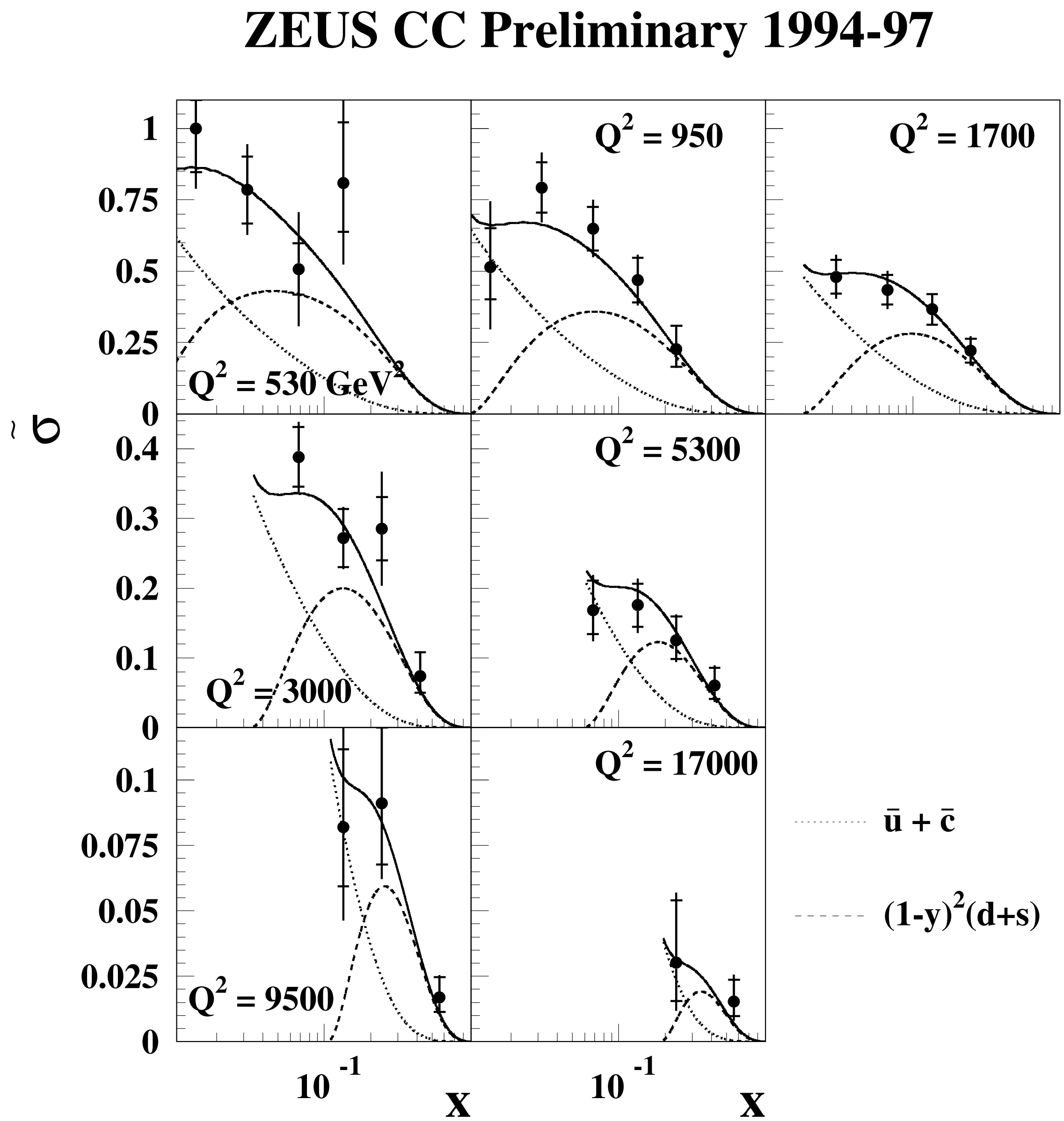

- Standard Model gives a good description of the CC cross-section
- d valence dominates at high x
- sea quarks dominate at low x

Can we measure the u/d ratio?

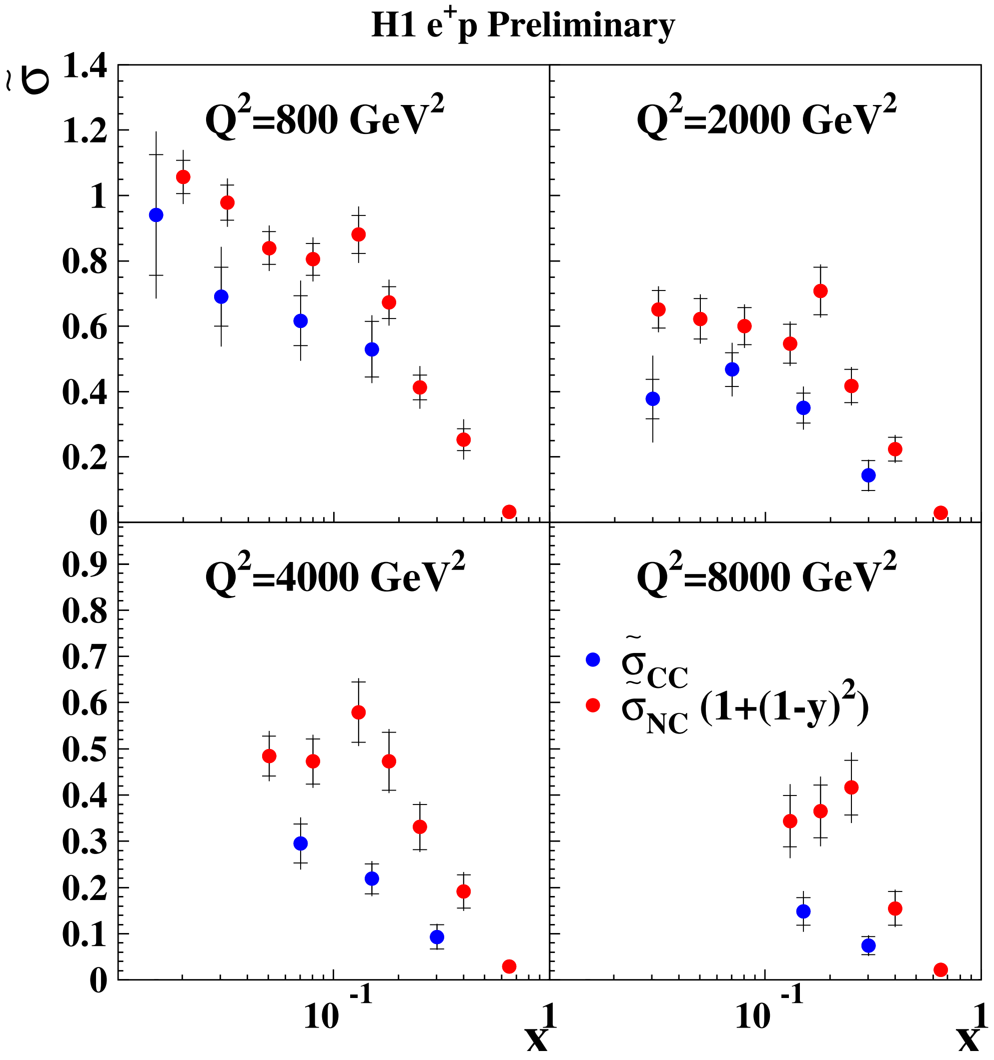

- neglecting xF_3, the S. F. term in L.O corresponds to:

$$\begin{array}{lll} & 1+(1-y)^2\left(\frac{4}{9}u+\frac{1}{9}d\right) & \text{in NC} \\ & (1-y)^2 d & \text{in CC} \\ \text{at 2000 GeV}^2\text{:} & \Leftrightarrow \quad 0.83\left(u+\frac{1}{4}d\right) & \text{in NC} \\ & \Leftrightarrow \quad 0.86 \quad d & \text{in CC} \end{array}$$

$$\boxed{\Rightarrow \mathbf{u/d} \sim 2}$$

Neutral and Charged Current Cross-Section

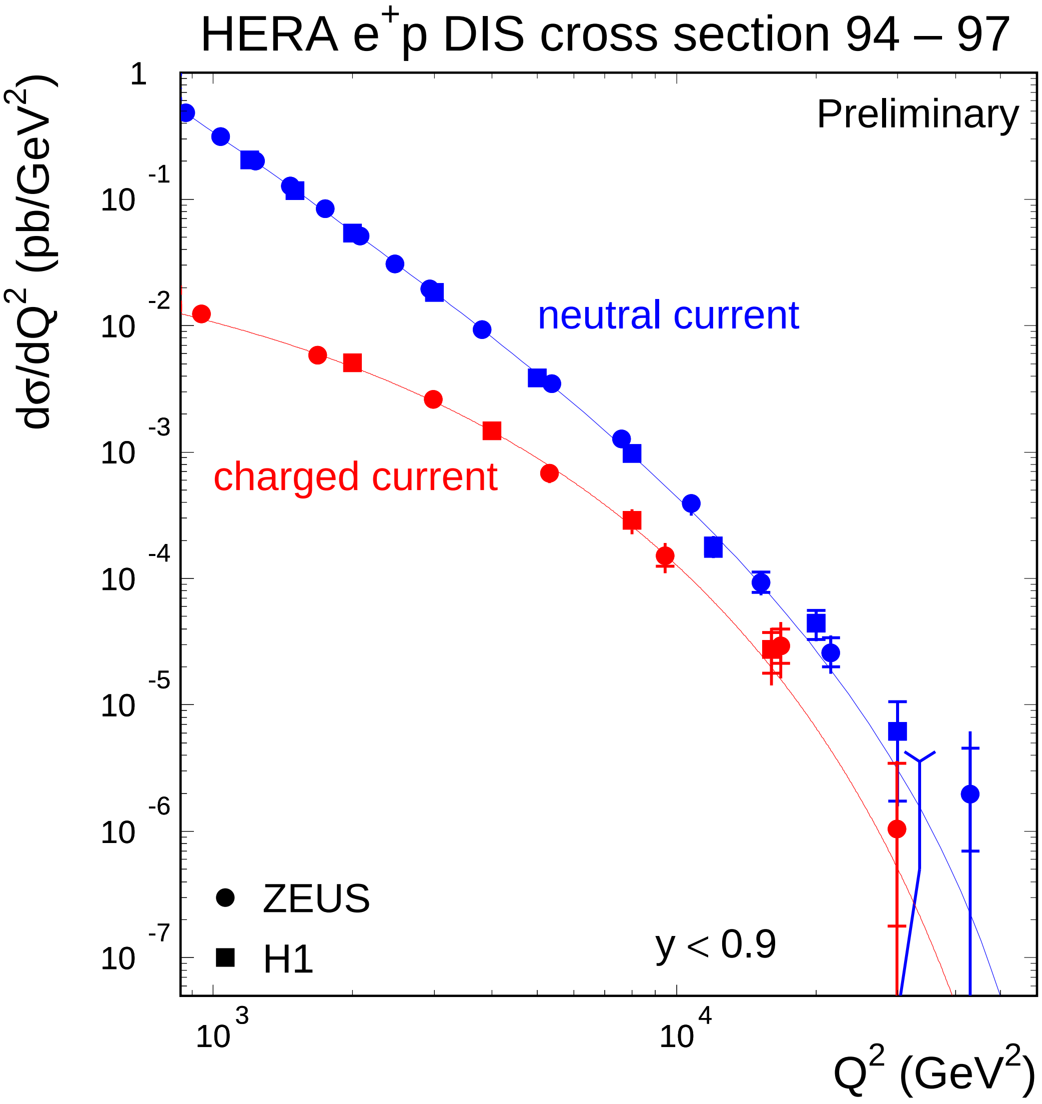

- Neutral and Charged Current Cross-Section have similar values at high Q^2
- remaining difference at high Q^2 are due to coupling to different quark flavours
- What happens at very high $Q^2 (\geq 15000\ \mathrm{GeV}^2)$?

Summary

- In its first years of operation, HERA has been testing the SM, in particular QCD and the Proton Structure, in new kinematic domains.
- More is coming with the expected 50 pb^{-1} of e^-p data in 98-99 which will complement the e^+p results presented here:

$\Rightarrow$ α_S, xg, p.d.f. measured precisely
$\Rightarrow$ hadronic final state studied in detail
$\Rightarrow$ check the excess at high Q^2 in e^-p

But also afterwards with the luminosity upgrade of HERA and its detectors in 2000. Between 2000 and 2005, 500-1000 pb^{-1} are expected.

Program will continue with higher precision and with an extended search potential

Surprises?

see U. Katz talk!!!